Title

Phosphorylation of Cav1.2 on S1928 uncouples the L-type Ca2+ channel from the β2 adrenergic receptor

Journal

The EMBO Journal, 35(12)

ISSN

0261-4189

Authors

Patriarchi, Tommaso
Qian, Hai
Di Biase, Valentina
et al.

Publication Date

2016-06-15

DOI

10.15252/embj.201593409

Peer reviewed

Article

TRANSPARENT PROCESS

THE EMBO JOURNAL

Phosphorylation of $Ca_v1.2$ on S1928 uncouples the L-type Ca^{2+} channel from the β_2 adrenergic receptor

Tommaso Patriarchi[1], Hai Qian[2], Valentina Di Biase[3], Zulfiquar A Malik[1,2], Dhrubajyoti Chowdhury[1], Jennifer L Price[1], Erik A Hammes[1], Olivia R Buonarati[1], Ruth E Westenbroek[4], William A Catterall[4], Franz Hofmann[5], Yang K Xiang[1], Geoffrey G Murphy[6], Chao-Ye Chen[1], Manuel F Navedo[1] & Johannes W Hell[1,2,*]

Abstract

Agonist-triggered downregulation of β-adrenergic receptors (ARs) constitutes vital negative feedback to prevent cellular overexcitation. Here, we report a novel downregulation of β_2AR signaling highly specific for $Ca_v1.2$. We find that β_2-AR binding to $Ca_v1.2$ residues 1923–1942 is required for β-adrenergic regulation of $Ca_v1.2$. Despite the prominence of PKA-mediated phosphorylation of $Ca_v1.2$ S1928 within the newly identified β_2AR binding site, its physiological function has so far escaped identification. We show that phosphorylation of S1928 displaces the β_2AR from $Ca_v1.2$ upon β-adrenergic stimulation rendering $Ca_v1.2$ refractory for several minutes from further β-adrenergic stimulation. This effect is lost in S1928A knock-in mice. Although AMPARs are clustered at postsynaptic sites like $Ca_v1.2$, β_2AR association with and regulation of AMPARs do not show such dissociation. Accordingly, displacement of the β_2AR from $Ca_v1.2$ is a uniquely specific desensitization mechanism of $Ca_v1.2$ regulation by highly localized β_2AR/cAMP/PKA/S1928 signaling. The physiological implications of this mechanism are underscored by our finding that LTP induced by prolonged theta tetanus (PTT-LTP) depends on $Ca_v1.2$ and its regulation by channel-associated β_2AR.

Keywords adrenergic receptors; glutamate receptors; L-type calcium channels; protein kinase A

Subject Categories Neuroscience

DOI 10.15252/embj.201593409 | Received 31 October 2015 | Revised 23 March 2016 | Accepted 24 March 2016 | Published online 22 April 2016

The EMBO Journal (2016) 35: 1330–1345

Introduction

Norepinephrine in the brain is important for arousal, behavioral acuity, and learning in novel and emotionally charged situations (Cahill *et al*, 1994; Berman & Dudai, 2001; Hu *et al*, 2007; Minzenberg *et al*, 2008; Carter *et al*, 2010). It signals via β_1 and β_2AR–G_s–adenylyl cyclase–cAMP–PKA cascades (Sanderson & Dell'Acqua, 2011). The β_2AR uniquely binds directly to the C-terminus of $\alpha_1$1.2, the central pore-forming subunit of $Ca_v1.2$ (Davare *et al*, 2001; Balijepalli *et al*, 2006), and via PSD-95 and auxiliary TARP subunits to AMPA-type glutamate receptors (AMPARs) (Joiner *et al*, 2010; see also Wang *et al*, 2010). These complexes also contain G_s (Davare *et al*, 2001; Joiner *et al*, 2010), adenylyl cyclase (Davare *et al*, 2001; Efendiev *et al*, 2010; Joiner *et al*, 2010; Nichols *et al*, 2010), and AKAP-anchored PKA (Davare *et al*, 2001; Tavalin *et al*, 2002; Hulme *et al*, 2003, 2006a; Hall *et al*, 2007; Oliveria *et al*, 2007; Joiner *et al*, 2010; Zhang *et al*, 2013; Dittmer *et al*, 2014). Assembly of such complexes brings all components of this cAMP cascade into close proximity with each other (Fig EV1A and B), which results in localized cAMP signaling and regulation of β_2AR-associated $Ca_v1.2$ and AMPAR (Chen-Izu *et al*, 2000; Davare *et al*, 2001; Hulme *et al*, 2003; Joiner *et al*, 2010). Spatial restriction of cAMP production, diffusion, and signaling is a key mechanism thought to underlie the specific cAMP effects seen for certain G_s protein-coupled receptors (G_sPCRs) (Smith *et al*, 2006; Leroy *et al*, 2008; Dai *et al*, 2009; Richter *et al*, 2013) including β_2AR (Jurevicius & Fischmeister, 1996; Kuschel *et al*, 1999; Chen-Izu *et al*, 2000; Davare *et al*, 2001; Balijepalli *et al*, 2006; Nikolaev *et al*, 2010). This localized signaling is in contrast to the broad non-target selective signaling by the β_1AR and other G_sPCRs (Xiao *et al*, 1999b; Steinberg & Brunton, 2001; Balijepalli *et al*, 2006). Despite much effort to prove this concept, clear evidence in

1 Department of Pharmacology, University of California, Davis, CA, USA
2 Department of Pharmacology, University of Iowa, Iowa City, IA, USA
3 Institute for Biophysics, Medical University of Graz, Graz, Austria
4 Department of Pharmacology, University of Washington, Seattle, WA, USA
5 Department of Pharmacology and Toxicology, Technical University of Munich, Munich, Germany
6 Department of Molecular & Integrative Physiology, Molecular & Behavioral Neuroscience Institute, University of Michigan, Ann Arbor, MI, USA
*Corresponding author. Tel: +1 530 752 6540; Fax: +1 530 752 7710; E-mail: jwhell@ucdavis.edu

support of this hypothesis as provided here by the effects of acute β_2AR displacement from $Ca_v1.2$ by peptide and S1928 phosphorylation (see below) has been lacking so far.

$Ca_v1.2$ is the most abundant L-type Ca^{2+} channel in brain and heart (Hell *et al*, 1993a). Mutations in $Ca_v1.2$ affect many tissues indicating widespread prominent $Ca_v1.2$ functions, which include control of cardiac contractility and heart rate as well as autistic-like behaviors (Splawski *et al*, 2004). Besides their prominent roles in cardiovascular function, L-type channels are critical in the brain for long-term potentiation (Grover & Teyler, 1990; Moosmang *et al*, 2005) and depression (LTD) (Bolshakov & Siegelbaum, 1994), neuronal excitability (Marrion & Tavalin, 1998; Berkefeld *et al*, 2006), and gene expression (Dolmetsch *et al*, 2001; Marshall *et al*, 2011; Li *et al*, 2012; Ma *et al*, 2014). Upregulation of $Ca_v1.2$ activity by β-adrenergic signaling is a central mechanism of regulating Ca^{2+} influx into cardiomyocytes (Reuter, 1983; Balijepalli *et al*, 2006) and neurons (Gray & Johnston, 1987; Davare *et al*, 2001; Oliveria *et al*, 2007; Dittmer *et al*, 2014). The differential global versus local regulation of $Ca_v1.2$ by β_1AR versus β_2AR might be due to association of the β_2AR but not β_1AR with $Ca_v1.2$ (Chen-Izu *et al*, 2000; Davare *et al*, 2001; Balijepalli *et al*, 2006). We now provide clear evidence for this notion by showing that acute displacement of the β_2AR by a peptide and by S1928 phosphorylation prevents phosphorylation and upregulation of $Ca_v1.2$ by β_2AR stimulation.

The most prominent and heavily regulated PKA phosphorylation site in $Ca_v1.2$ is S1928 in the C-terminus of its central $\alpha_1$1.2 subunit (Hell *et al*, 1993b, 1995; De Jongh *et al*, 1996; Davare *et al*, 1999, 2000; Davare & Hell, 2003; Hulme *et al*, 2006a; Hall *et al*, 2007; Dai *et al*, 2009). However, functional studies argue against S1928 regulating channel activity in the heart (Ganesan *et al*, 2006; Lemke *et al*, 2008). Here, we found that the β_2AR binds to $\alpha_1$1.2 residues 1923–1942 and that S1928 phosphorylation within this segment disrupts this interaction. This mechanism constitutes a particular form of downregulation of β_2AR signaling upon prolonged stimulation that specifically blunts subsequent upregulation of $Ca_v1.2$ but not AMPAR phosphorylation and activity and is absent in S1928A knock-in mice.

Results

The β_2AR binds to residues 1923–1942 in the C-terminus of $Ca_v1.2$

As the β_2AR C-terminus mediates binding to $Ca_v1.2$ (Davare *et al*, 2001), we utilized amylose-immobilized maltose-binding protein (MBP)-tagged β_2AR C-terminus in pull-down experiments to define its binding site in $\alpha_1$1.2. We first tested affinity purified glutathione S-transferase (GST) fusion proteins of the N-terminus of $\alpha_1$1.2, the three loops between the four homologous membrane domains of $\alpha_1$1.2, and the three C-terminal constructs CT1 (aa 1507–1733), CT23 (aa 1622–1905), and CT4 (aa 1909–2171), which cover the whole $\alpha_1$1.2 C-terminus (Fig 1A). From these constructs, only CT4 bound to the MBP-tagged β_2AR C-terminus, indicating a highly specific interaction (Fig 1B and C). From three fragments that covered CT4 (CTC (aa 1834–1957); CTD (aa 1944–2067); CTE (aa 2054–2171)), only CTC bound to the β_2AR (Fig 1D and E). These results restrict the interaction site to the overlapping region between CTC and CT4 (aa 1909–1957).

To test whether CT4 and CTC bind to native $Ca_v1.2$ and could be used to acutely and specifically disrupt the β_2AR–$Ca_v1.2$ complex, the β_2AR was immunoprecipitated in the absence and presence of CT4 and CTC and, as negative controls, CT1, CT23, and CTD. CT4 and CTC but not the other polypeptides completely displaced $Ca_v1.2$ from the β_2AR (Fig 1F, G and I). To eliminate the possibility of nonspecific or secondary effects of the polypeptides on the complex, we monitored within the same samples and same immunoblot lanes co-immunoprecipitation (co-IP) of the AMPAR subunit GluA1, which forms a separate complex with the β_2AR. In contrast to $Ca_v1.2$, this interaction is mediated by PDZ interactions with PSD-95 (Fig EV1A and B), and therefore, neither CT4 nor CTC affected the GluA1–β_2AR co-IP (Fig 1F and H).

To further narrow down the β_2AR binding site of $\alpha_1$1.2, synthetic peptides covering aa 1906–1925 (Pep 1), aa 1923–1942 (Pep 2), and aa 1939–1959 (Pep 3) whose N-termini were labeled with fluorescein (FITC), were titrated with the β_2AR C-terminus, and their binding was monitored by fluorescence polarization. Pep2, but neither Pep1 nor Pep3, showed strong and saturable binding with an apparent K_d of ~1.9 μM (Fig 2A). In addition, only Pep2 displaced $\alpha_1$1.2 (but not GluA1) from the β_2AR during IP (Fig 2B–D).

Unlabeled synthetic Pep2 and synthetic Pep2 with S1928 being phosphorylated (PhPep2) were added during IP of β_2AR to test whether phosphorylation of S1928 affects β_2AR binding. While Pep2 removed $Ca_v1.2$ (but, once more, not GluA1), PhPep2 had no effect suggesting that S1928 phosphorylation impairs β_2AR binding (Fig 2E and F).

S1928 phosphorylation displaces the β_2AR from $Ca_v1.2$

To evaluate whether S1928 phosphorylation displaces the β_2AR from $Ca_v1.2$, we monitored $Ca_v1.2$ phosphorylation and β_2AR–$Ca_v1.2$ association in forebrain slices upon stimulation with the βAR agonist isoproterenol (ISO). S1700 has recently emerged as a PKA phosphorylation site that is important for upregulation of $Ca_v1.2$ activity in heart (Fuller *et al*, 2010; Hell, 2010; Fu *et al*, 2013). As phosphorylation of S1700 and S1928 increased (Fig 3A–C), association of $Ca_v1.2$ with the β_2AR decreased (Fig 3D and E). Strikingly, no such decrease was observed in slices from S1928A KI mice, even though ISO induced S1700 phosphorylation in these mice (Fig 3G–K). Displacement of the β_2AR from $Ca_v1.2$ is unique for S1928 phosphorylation, as the β_2AR–GluA1 interaction was not disrupted by ISO application (Fig 3D, F, J and L), which induced phosphorylation of S845 (Fig EV1C and D), a well-established PKA site on GluA1 (Roche *et al*, 1996). IP of $Ca_v1.2$ followed by IB of β_2AR confirmed their dissociation upon ISO treatment in WT but not S1928A KI mice (Fig 3A, bottom; Fig EV1F and G).

To test whether the ISO-induced dissociation of the β_2AR from $Ca_v1.2$ results in their spatial separation, we co-expressed $\alpha_1$1.2 with the HA tag within an extracellular loop ($\alpha_1$1.2-HA) and β_2AR with the FLAG tag at its extracellular N-terminus (FLAG-β_2AR) in cultured hippocampal neurons. Line scan analysis of the fluorescence distribution of the surface labeled $\alpha_1$1.2-HA and FLAG-β_2AR (see Appendix Supplementary Methods) showed that the median distance between neighboring $\alpha_1$1.2-HA and FLAG β_2AR clusters significantly increases from 0.24 μm (25–75% interquartile range: 0.15–0.44 μm) to 0.34 μm (IQR: 0.21–0.54 μm) after 5 min of ISO treatment (Fig 4). Because the distribution of distances failed two normality tests (see

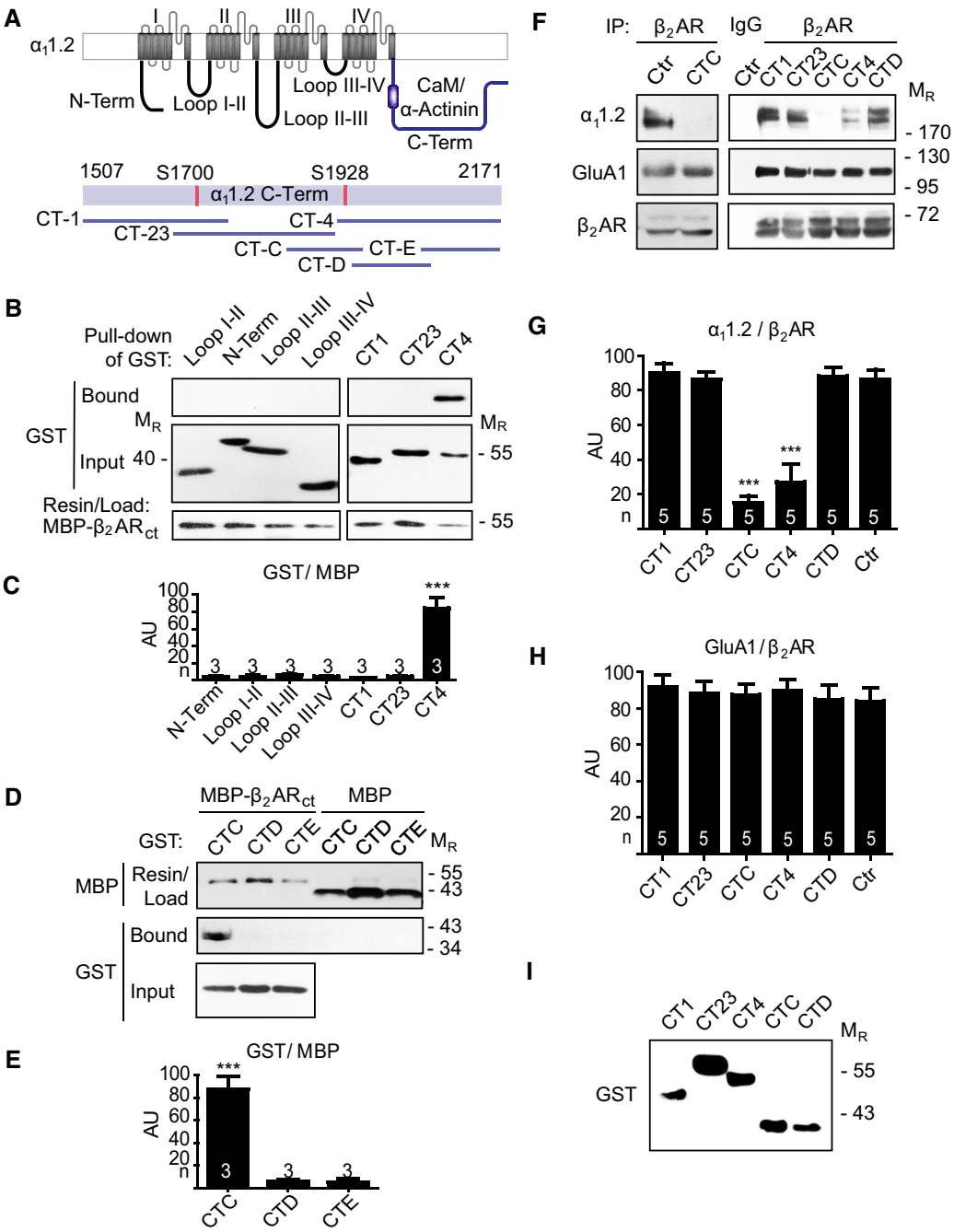

Figure 1. Identification of the β_2AR binding region on $Ca_v1.2$.

A Schematic of the $\alpha_1$1.2 subunit of $Ca_v1.2$ (top) and the $\alpha_1$1.2-derived GST fusion proteins covering the C-terminus (bottom).

B Pull-down of GST-tagged $\alpha_1$1.2 segments (top immunoblot; IB) by immobilized MBP-β_2AR C-terminus (residues 326–413 of human β_2AR). GST fusion proteins were detected by an anti-GST antibody and MBP fusion proteins by an anti-MBP antibody. Middle IB shows that comparable amounts of the various GST fusion proteins had been added to the resin samples and bottom IB illustrates equal loading of all amylose resin samples with MBP-β_2AR.

C Quantification of (B).

D Pull-down of GST-CTC but not GST-CTD or GST-CTE (middle IB) by immobilized MBP-β_2AR C-terminus (left) but not MBP alone (right), all of which were present at comparable amounts (bottom and top IBs, respectively). GST fusion proteins were detected by an anti-GST antibody and MBP fusion proteins by an anti-MBP antibody.

E Quantification of (D).

F IP of β_2AR in the presence of 10 μM GST (Control; Ctr) or GST-tagged C-terminal fragments as indicated. CT4 and CTC specifically displaced $\alpha_1$1.2 (top of IB) but not GluA1 (middle of same IB) from β_2AR (bottom of same IB). Use of non-specific IgG (left lane in right panels) indicates specificity of IP.

G, H For quantification of coIPs, $\alpha_1$1.2 (G) and GluA1 (H) immunosignals from (F) were normalized to β_2AR signals.

I Representative IB showing amounts of the GST fusion proteins that were added in (F), as detected by anti-GST antibodies.

Data information: Data are presented as mean ± SEM. $n = 3$ (C, E) or 5 (G, H). ***$P < 0.001$, one-way ANOVA.

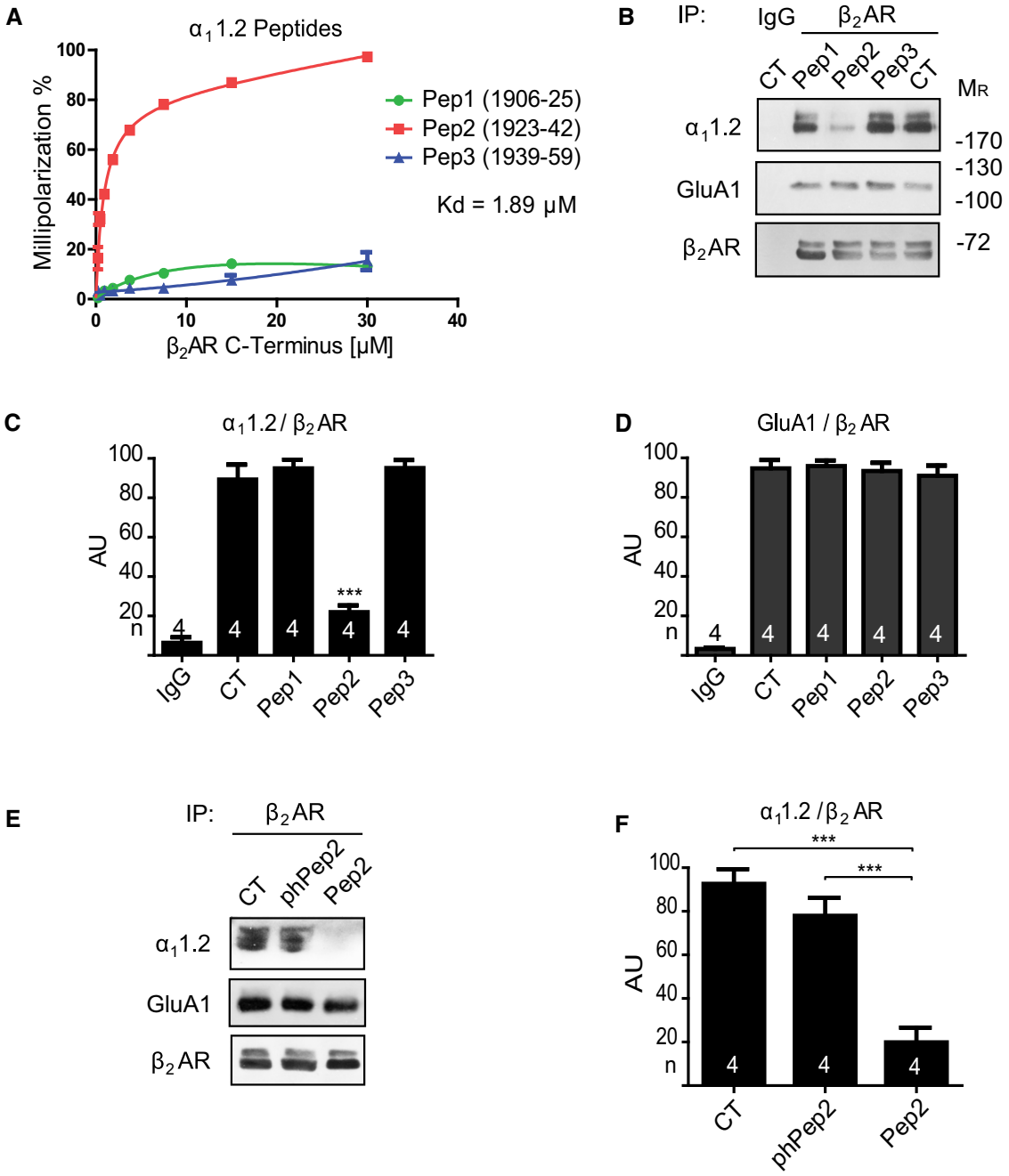

Figure 2. The β_2AR binds to the S1928 phosphorylation site.

A Titration of fluorescence polarization of FITC peptides (100 nM) spanning $\alpha_1$1.2 aa 1906–1959 with purified MBP-β_2AR C-terminus. K_d value was obtained by fitting a nonlinear direct binding curve to Pep2.

B IP of β_2AR in the absence (Control) or presence of 10 µM peptides, as indicated. Pep2 specifically displaced $\alpha_1$1.2 (top of IB) but not GluA1 (middle, same IB) from β_2AR (bottom, same IB). Use of non-specific IgG (left lane) indicates specificity of (co)IPs.

C, D For quantification, $\alpha_1$1.2 (C) and GluA1 (D) IB signals from (B) were normalized to β_2AR signals.

E IP of β_2AR in the absence (Control) or presence of 10 µM Pep2 or Pep2 with S1928 being phosphorylated (phPep2), which did not displace $\alpha_1$1.2.

F $\alpha_1$1.2 IB signals were normalized to β_2AR signals.

Data information: Data are presented as mean ± SEM. $n = 4$. ***$P < 0.001$, one-way ANOVA.

Appendix Supplementary Methods), we used the nonparametric Mann–Whitney Rank test for statistical analysis, which resulted in a two-tailed P-value of < 0.0001. The Kolmogorov–Smirnov cumulative distributions test yielded a P-value < 0.0001. In addition, Pearson's correlation analysis yielded a coefficient 0.36 ± 0.03 (mean ± SEM) for control and 0.29 ± 0.02 for ISO treated neurons with $P = 0.037$. Furthermore, we calculated the fraction of overlap between $Ca_V1.2$-HA and FLAG-β_2AR puncta. We obtained a

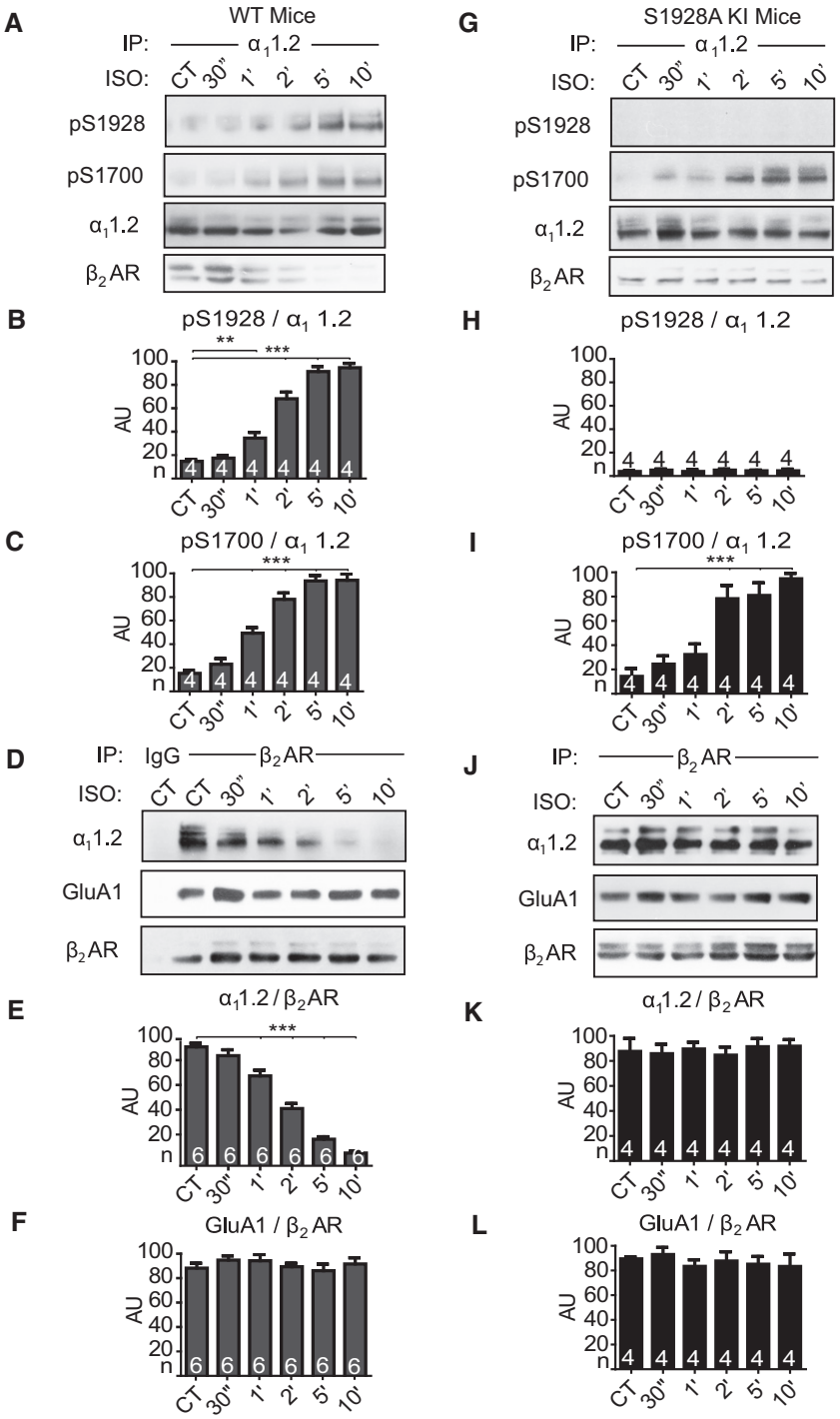

Figure 3. S1928 phosphorylation displaces β_2AR from $Ca_v1.2$.

Forebrain slices from WT (A–F) and S1928A KI mice (G–L) were treated with vehicle (water) or 10 μM isoproterenol (ISO) for 0.5–10 min before solubilization, ultracentrifugation, IP of $\alpha_1$1.2 (A–C, G–I) or β_2AR (D–F, J–L), and sequential IB for pS1928, pS1700, and $\alpha_1$1.2, for GluA1, or for β_2AR, of corresponding regions of the blots, as indicated. All the $\alpha_1$1.2 IPs in (A–C) and (G–I) were from the same samples (which were split in half for parallel IP) as the β_2AR IPs in (D–F) and (J–L), respectively (for quantification of coIP of β_2AR with $\alpha_1$1.2 see Fig EV1F and G).

A–F In WT, the time-dependent increase in S1928 and S1700 phosphorylation (A–C) paralleled the decrease in coIP of β_2AR with $\alpha_1$1.2 (A bottom, Fig EV1F) and of $\alpha_1$1.2 with β_2AR (D–F). For quantification of $\alpha_1$1.2 phosphorylation (B, C), pS1928 and pS1700 signals were normalized to $\alpha_1$1.2. For quantification of coIP (E, F), $\alpha_1$1.2 and GluA1 signals were normalized to β_2AR.

G–L In S1928A KI mice, ISO induced S1700 phosphorylation (G, I) but did not disrupt the $\alpha_1$1.2–β_2AR interaction (G bottom, J–L, Fig EV1G). For quantification of $\alpha_1$1.2 phosphorylation (H, I), pS1928 and pS1700 signals were normalized to $\alpha_1$1.2. For quantification of coIP (K, L), $\alpha_1$1.2 and GluA1 signals were normalized to β_2AR.

Data information: Data are presented as mean ± SEM. n = 4 (B, C, H, I, K and L) or 6 (E, F). $^{**}P < 0.01$, $^{***}P < 0.001$, one-way ANOVA.

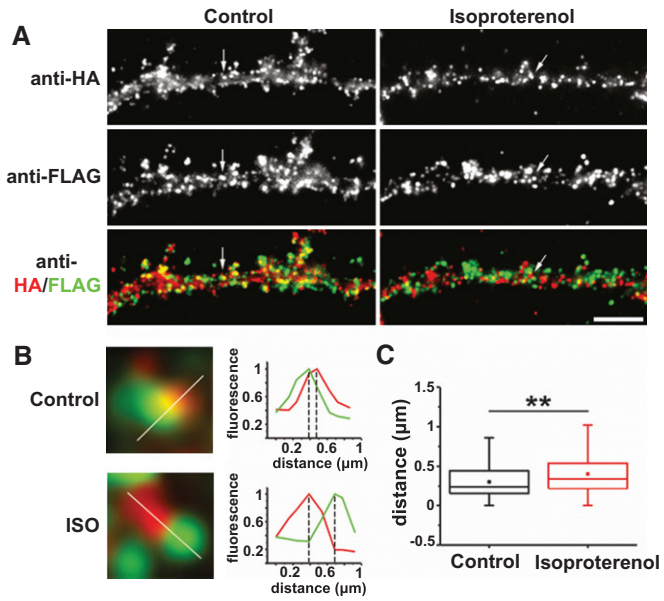

Figure 4. S1928 phosphorylation separates β_2AR from $Ca_v1.2$.
Hippocampal cultures were transfected with FLAG-β_2AR and $\alpha_1$1.2-HA at 6 days *in vitro* (DIV), treated with vehicle (water) or 1 μM isoproterenol (ISO) for 5 min at 18 DIV, fixed and surface labeled for HA and FLAG.

A, B Representative immunofluorescent images obtained by wide-field microscopy at lower and higher resolutions (scale bar, 5 μm). Arrows in (A) indicate the samples enlarged in (B).

C Quantification of distance between centers of HA and FLAG puncta (**$P < 0.001$, Mann–Whitney rank sum test). The bars represent 5th (lower end) and 95th percentile (higher end).

Mander's coefficient of 0.41 ± 0.03 (mean ± SEM) for control and 0.31 ± 0.03 for ISO treated neurons with $P = 0.02$. These results are consistent with the idea that ISO stimulation displaces the β_2AR from $Ca_v1.2$.

ISO-triggered dissociation of the β_2AR from $Ca_v1.2$ prevents subsequent $Ca_v1.2$ phosphorylation

Could the displacement of the β_2AR from $Ca_v1.2$ upon S1928 phosphorylation be a novel mechanism that specifically downregulates this powerful β adrenergic regulation of Ca^{2+} influx into neurons? To test this idea at the molecular level, forebrain slices from WT mice were treated with vehicle or ISO for 5 min, followed by washout of ISO for various time periods before re-application of ISO. 20-min and even 10-min but not 3-min washout reversed the ISO-induced displacement of the β_2AR from $\alpha_1$1.2 (Fig 5A, lane 5 vs. 7; Fig EV2A–C). S1700 and S1928 phosphorylation returned to baseline already after 3-min washout (Fig 5D, lanes 2–4; Fig 5E and F). As expected, phosphorylation of GluA1 on S845 behaved similarly (Fig 5D and G); phosphorylation of S831, which can be mediated by PKC and CaMKII but not PKA (Roche *et al*, 1996; Halt *et al*, 2012), served as a negative control that is inert to PKA stimulation (Fig 5D and H).

We tested whether the acute displacement of the β_2AR from $\alpha_1$1.2 affects re-phosphorylation and re-stimulation of $Ca_v1.2$ after 3-min washout. In fact, re-application of ISO after a 3-min washout was not able to induce a second round of phosphorylation of S1700 or S1928 (Fig 5D, lane 6). In contrast, in mock washout samples ISO was fully effective in inducing phosphorylation of these residues following initial application of vehicle instead of ISO before the 3-min washout (Fig 5D, lane 5). The ISO-induced displacement of the β_2AR from $\alpha_1$1.2 was specific for $Ca_v1.2$, as coIP of GluA1 with the β_2AR was not affected within same samples that were analyzed for $Ca_v1.2$ coIP (Fig 5A and C). Re-phosphorylation of S845 during the second ISO treatment was also not blunted by the first ISO application (Fig 5D, lane 6; Fig 5G). Accordingly, displacement of the β_2AR from $Ca_v1.2$ selectively downregulates the signaling pathway from the β_2AR to $Ca_v1.2$ without affecting another target, GluA1, which also forms a signaling complex with the β_2AR. To test whether endocytosis of the β_2AR is responsible for lack of re-phosphorylation of $\alpha_1$1.2 by the second ISO application, we blocked endocytosis with two different drugs, dynasore and pitstop. Neither affected the loss of $\alpha_1$1.2 phosphorylation by the second ISO pulse (Fig EV3) arguing against this possibility.

Strikingly, in S1928A KI mice, re-phosphorylation of S1700 during the second ISO application after 3-min washout was not decreased at all as compared to single ISO applications (Fig 6A, lane 6 vs. lanes 2 and 5). In fact, the second ISO treatment appears to have increased S1700 phosphorylation more strongly than the first treatment. These results suggest that additional, as yet to be identified, mechanisms exist that enhance phosphorylation of S1700 during repetitive activation of β_2AR bound to $Ca_V1.2$. For instance, like PKA, the phosphatase PP2B/calcineurin is linked to $Ca_V1.2$ via AKAP5 to counteract $Ca_V1.2$ phosphorylation by PKA (Oliveria *et al*, 2007; Fuller *et al*, 2014; Murphy *et al*, 2014) but released upon elevated Ca^{2+} influx via $Ca_V1.2$ (Li *et al*, 2012; Murphy *et al*, 2014). Because β adrenergic stimulation will increase Ca^{2+} influx via $Ca_V1.2$ as occurring under basal conditions due to neuronal network activity (Hall *et al*, 2013), it is conceivable that PP2B is displaced from $Ca_V1.2$ for 3 min or longer, allowing for stronger phosphorylation of S1700 in S1928A KI neurons upon ISO application that is repeated within 3 min.

The ISO-induced displacement of the β_2AR from $\alpha_1$1.2 is completely reversible, as 10-min washout of ISO resulted in full coIP of $\alpha_1$1.2 with the β_2AR (Fig 5A, lane 7; Fig EV2A–C), which is preceded by dephosphorylation of S1928 and also S1700 (Fig EV2D). A 20-min washout also restored the capability of the β_2AR to induce S1700 and S1928 phosphorylation (Fig EV3A and B, compare lanes 2 and 3).

ISO-triggered dissociation of the β_2AR from $Ca_v1.2$ prevents subsequent stimulation of L-type channel activity

To functionally test whether β_2AR stimulation affects subsequent regulation of $Ca_v1.2$ by a second, closely timed pulse of β_2AR stimulation, we sought to record single-channel L-type currents from cultured neurons in the cell-attached patch clamp mode as in our previous work (Davare *et al*, 2001). Other Ca^{2+} channels were blocked by adding specific inhibitors (ωCTxGVIA and ωCTxMVIIC) to the patch pipette solution. We determined open probability (Po) from all channels within each patch (NPo) in recordings from neurons with either vehicle or ISO added to the patch pipette. Figure 7A shows original traces with single-channel activity elicited by depolarizing pulses from −80 mV to several test potentials. These data were fit with a linear function that revealed a slope conductance

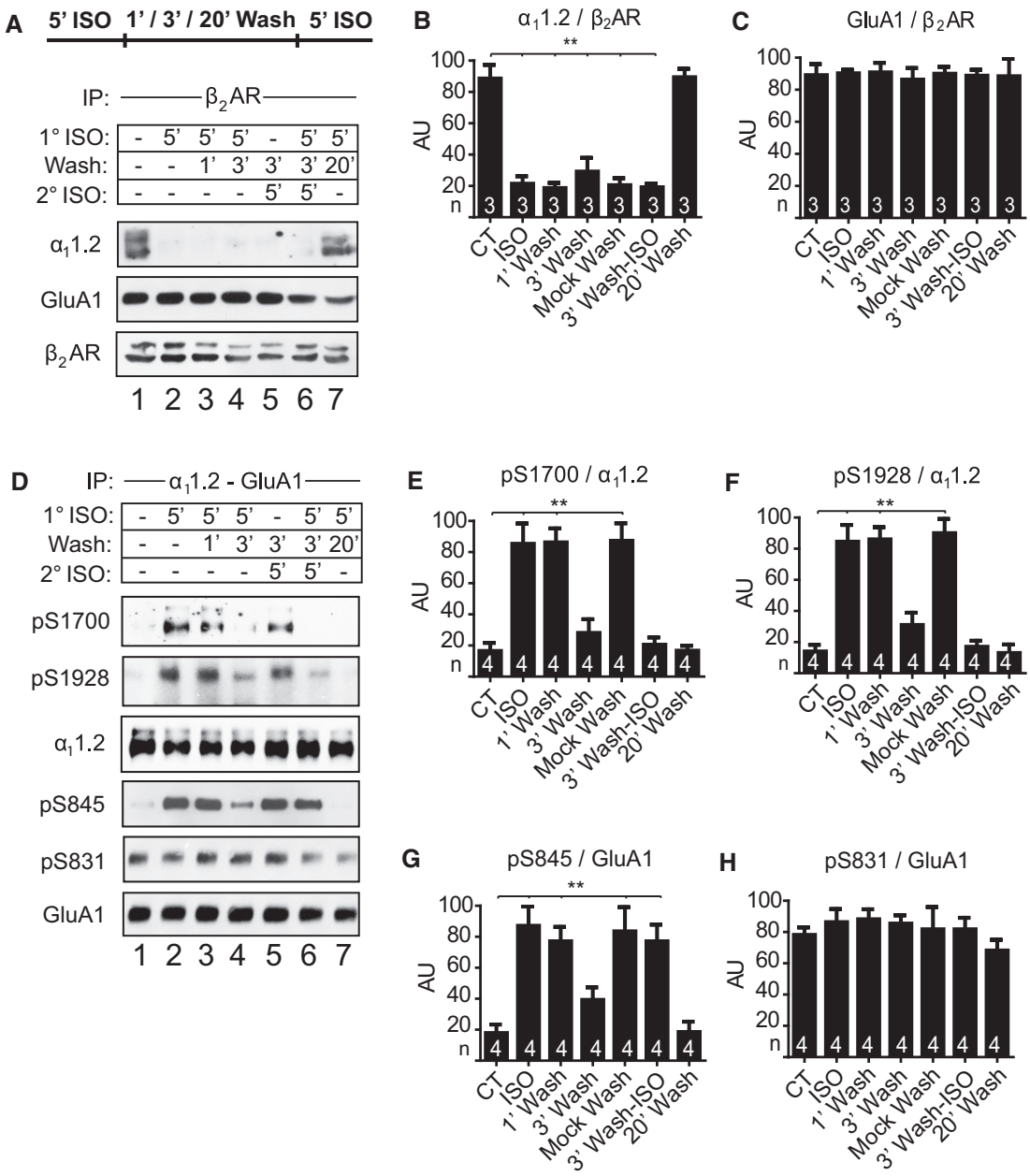

Figure 5. ISO-induced displacement of the β_2AR from $Ca_v1.2$ blunts subsequent $Ca_v1.2$ phosphorylation.

Forebrain slices from WT mice were treated with vehicle (water; lanes 1, 5; numbers on bottom) or 10 μM ISO for 5 min, followed, if indicated, by 1-min, 3-min, or 20-min washout of ISO (lanes 3–7) and a second application of ISO for 5 min (lane 6), before solubilization and ultracentrifugation.

A β_2AR was IPed before IB for $\alpha_1$1.2 (top part of IB), GluA1 (middle part of IB), and β_2AR (bottom part of IB), as indicated. ISO-induced displacement of the β_2AR from $\alpha_1$1.2 (lanes 2–6) lasted at least 3 min but not 20 min (compare lanes 6 and 7).

B, C For quantification, $\alpha_1$1.2 (B) and GluA1 (C) IB signals from (A) were normalized to β_2AR.

D $\alpha_1$1.2 and GluA1 were concurrently IPed from same samples as in (A) by simultaneous addition of anti-$\alpha_1$1.2 and anti-GluA1 antibodies before probing and stripping/re-probing upper part of IB for pS1928, pS1700, and total $\alpha_1$1.2 (top three panels) and middle part for pS845, pS831, and total GluA1 (bottom three panels). ISO-induced displacement of the β_2AR from $\alpha_1$1.2 (see A) rendered $\alpha_1$1.2 (but not GluA1) refractory to re-phosphorylation of S1928 and S1700 upon a second ISO application of $\alpha_1$1.2 (compare lanes 5 and 6).

E–H For quantification, pS1700 (E) and pS1928 (F) IB signals from (D) were normalized to total $\alpha_1$1.2, and pS845 (G) and pS831 (H) signals from (D) to total GluA1.

Data information: Data are presented as mean ± SEM. $n = 3$ (B, C) or 4 (E–H). $^{**}P < 0.01$, one-way ANOVA.

for these channels of 27 ± 2 pS (Fig 7A), which corresponds to the expected slope conductance for an L-type $Ca_v1.2$ channel under similar experimental conditions (Yue & Marban, 1990). As expected, ISO significantly increased NPo (Fig 7B–D) without affecting single-channel amplitudes (see Appendix Fig S1) (Davare *et al*, 2001). Inclusion of the potent L-type channel blocker nifedipine abrogated

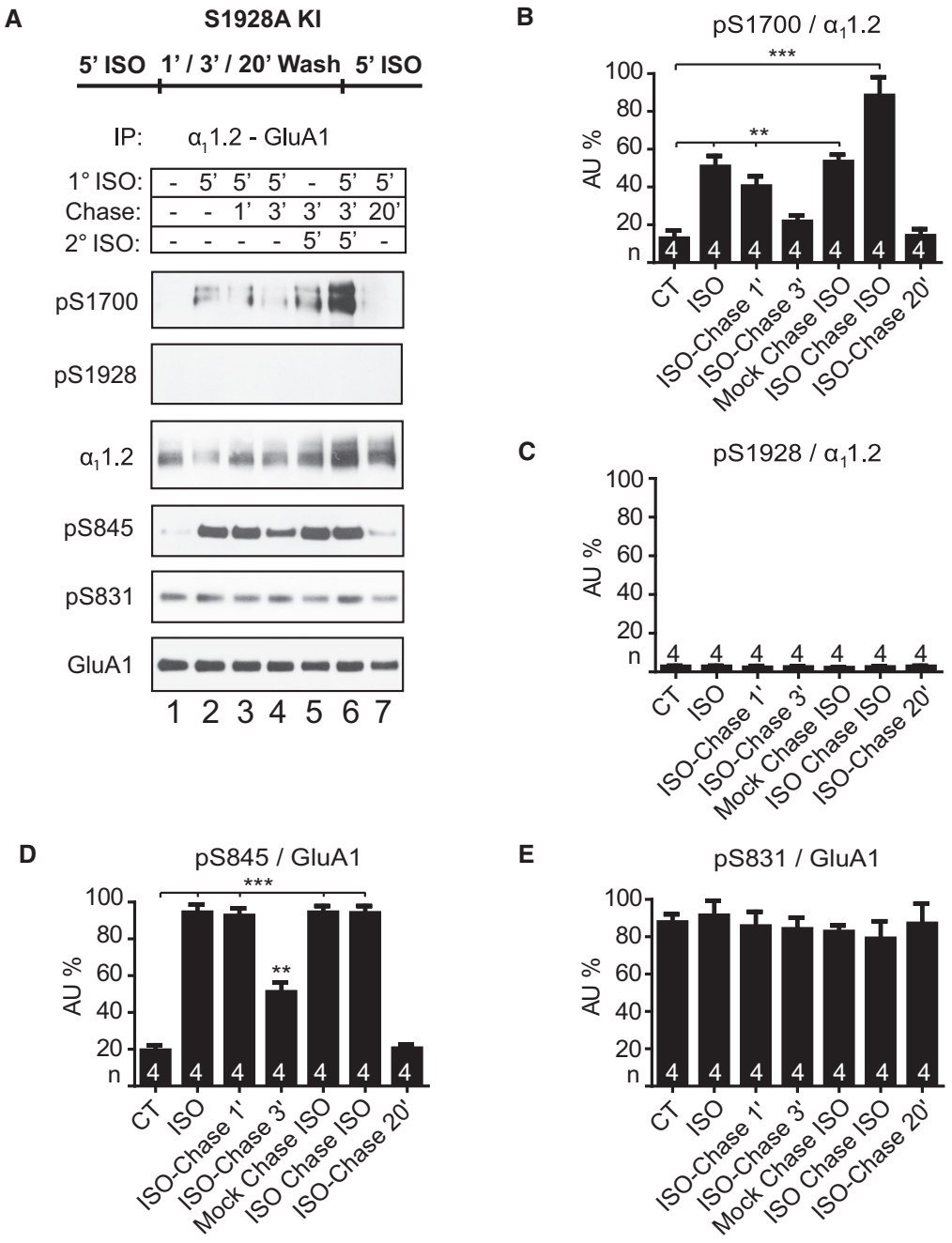

Figure 6. ISO pre-treatment does not blunt $Ca_V1.2$ phosphorylation by subsequent ISO treatment in S1928A KI mice.

Forebrain slices from S1928A KI mice were treated with vehicle (lanes 1, 5) or 10 μM ISO for 5 min, followed, if indicated, by 1-min, 3-min, or 20-min washout of ISO (lanes 3–7) and a second application of ISO for 5 min (lane 6), before solubilization and ultracentrifugation.

A $\alpha_1$1.2 and GluA1 were concurrently IPed from same samples by simultaneous addition of anti-$\alpha_1$1.2 and anti-GluA1 antibodies before probing and stripping/re-probing upper part of IB for pS1928, pS1700, and total $\alpha_1$1.2 and middle part for pS845, pS831, and total GluA1. In S1928A KI mice, S1700 re-phosphorylation after a 3-min washout of ISO was not blunted (lane 6) in contrast to WT mice but rather augmented (compare to lane 5).

B–E For quantification, pS1700 (B) and pS1928 (virtually absent) (C) IB signals from (A) were normalized to total $\alpha_1$1.2, and pS845 (D) and pS831 (E) signals from (A) to total GluA1.

Data information: Data are presented as mean ± SEM. $n = 4$. $^{**}P < 0.01$, $^{***}P < 0.001$, one-way ANOVA.

virtually all currents either with or without ISO present (Fig 7D). Hence, recordings reflect L-type currents under either condition. The ISO effect was prevented by the highly specific PKA-inhibitory PKI peptide, which carried 11 Arg residues to render it membrane permeant (Lu *et al*, 2007, 2011) (Fig 7D), thus confirming that the ISO-induced upregulation of L-type current is via PKA.

Most critically, when ISO was first applied to the bath for 5 min before washout and subsequent formation of a patch, the ISO included in the patch only upregulated L-type current when the washout was at least 10 min long (Fig 7E–H). If washout was only 3 min, channel activity remained low during the cell-attached recording with ISO in the patch pipette (Fig 7F and H). As expected, pre-treatment with vehicle followed by a 3-min washout (mock wash; Fig 7E and H) did not affect upregulation of channel activity by ISO in the patch pipette. Accordingly, sequential stimulation of L-type currents by two ISO applications was only effective if the interim time period was long enough to match the time frame required for the β_2AR to re-associate with $Ca_v1.2$ (Fig 5A, lanes 6 and 7, and C; Fig EV2A and C) and re-phosphorylate it (Fig EV3A, lane 3 vs. lane 2).

Binding of the β_2AR to residues 1923–1942 is required for β adrenergic stimulation of $\alpha_1$1.2 phosphorylation and $Ca_v1.2$ activity

To exclude the possibility that covert effects other than displacement of the β_2AR from $Ca_v1.2$ might be responsible for loss of sensitivity of channel activity to a second pulse of ISO, the β_2AR was acutely displaced from $Ca_v1.2$ by Myr-Pep2, a myristoylated version of Pep2, which mimics the binding site of aa 1923–1942 on the $\alpha_1$1.2 subunit and displaces the β_2AR from $Ca_v1.2$ (Fig 2). Myristoylation renders peptides membrane permeant. We first determined at which concentration Myr-Pep2 effectively disrupts the β_2AR–$Ca_v1.2$ interaction by adding increasing amounts to brain extracts during the IP of the β_2AR. 0.1–10 μM Myr-Pep2 increasingly displaced $Ca_v1.2$ from the β_2AR, with 10 μM being apparently 100% effective without affecting the β_2AR–GluA1 association (Fig EV4A–C).

Forebrain slices were incubated for 30 min with vehicle, 10 μM Myr-Pep2, Myr-Pep2scr, or Myr-DSPL. MyrPep2scr is a scrambled version of MyrPep2 and served as negative control. Myr-DSPL consists of the 14 aa at the very C-terminus of the β_2AR, which interacts with the third PDZ domain of PSD-95 (Joiner *et al*, 2010) (Fig EV1B). PSD-95 in turn is linked to a subset of AMPARs via its binding to the auxiliary AMPAR subunits known as γ subunits or TARPs, including stargazin (Stg/γ_2). Myr-DSPL specifically disrupts the interaction of the AMPAR subunit GluA1 with the β_2AR (Joiner *et al*, 2010) and served as a second negative control. In our experiments, Myr-Pep2 displaced $\alpha_1$1.2 but not GluA1 from the β_2AR (Fig 8A, compare lane 5 with 3; Fig 8B and C). In contrast, Myr-DSPL removed GluA1 but not $\alpha_1$1.2 from the β_2AR (Fig 8A, compare lane 1 with 3; Fig 8B and C). As before, ISO on its own caused a strong reduction in the coIP of $\alpha_1$1.2, but not GluA1, with the β_2AR (Fig 8A, compare lane 4 with 3; Fig 8B and C). In combination with ISO, Myr-Pep2 (compare lane 6 with 4) but not Myr-DSPL (compare lane 2 with 4) caused a virtually complete displacement of the β_2AR from $Ca_v1.2$. As a second control, Myr-Pep2scr had no effect on the association of the β_2AR with $Ca_v1.2$ whether slices were treated with ISO or not (Fig EV4D and E).

Importantly, the ISO-induced increase in phosphorylation of $\alpha_1$1.2 on S1700 (Fig 8D, lane 4 vs. 3, and E) was blocked by Myr-Pep2 (lanes 6 vs. 5) but not Myr-DSPL (lanes 1 vs. 2). The exact opposite was true for phosphorylation of GluA1 on S845 (Fig 8D and F). Accordingly, specific displacement of the β_2AR from $Ca_v1.2$ affects $Ca_v1.2$ but not GluA1 phosphorylation and vice versa. Furthermore, Myr-Pep2scr did not affect phosphorylation of either $\alpha_1$1.2 or GluA1 (Fig EV4G–J), confirming the specific actions of Myr-Pep2.

To define the functional consequences of disrupting the β_2AR–$Ca_v1.2$ interaction, in interleaved experiments cultured neurons were pre-incubated for 30 min with Myr-Pep2 or Myr-Pep2scr. Subsequent recording with ISO in the patch pipette indicated that Myr-Pep2 but not Myr-Pep2scr completely blocked the upregulation of channel function by ISO compared to vehicle controls (Fig 8G and H). We conclude that dissociation of the β_2AR–$Ca_v1.2$ complex by Myr-Pep2 prevents upregulation of $Ca_V1.2$ channel phosphorylation and activity.

The β_2AR–$Ca_v1.2$ interaction is required for PTT-LTP

Prolonged stimulation of the Schaffer collateral pathway at 5–10 Hz, which mimics the naturally occurring theta frequency (7 Hz), induces LTP (PTT-LTP) if at the same time β_2AR (but not β_1AR) are stimulated (Thomas *et al*, 1996; Hu *et al*, 2007; Qian *et al*, 2012). This potentiation develops over a period of 15 min with the first 5–10 min showing an initial depression (Thomas *et al*, 1996; Hu *et al*, 2007; Qian *et al*, 2012). Because β_2AR stimulation prominently augments Ca^{2+} influx through $Ca_v1.2$ at postsynaptic sites (Hoogland & Saggau, 2004), we tested whether $Ca_v1.2$ in general and specifically its upregulation by the β_2AR is required for PTT-LTP. In fact, PTT-LTP was completely absent in conditional knockout mice in which Cav1.2 had been deleted in glutamatergic forebrain neurons when compared to WT littermate controls (Fig 9A–C). Analysis of input–output relation and paired pulse facilitation indicated that synaptic transmission is normal in both genotypes (Fig EV5). In contrast to the 5 Hz PTT-LTP stimulus paradigm, LTP induced by a 100 Hz/1 s tetanus depends on NMDARs and not L-type channels. In this case, potentiation is very strong immediately after the tetanus in part due to presynaptic mechanisms but typically relaxes to a significantly lower level over ~5 min. This 100 Hz LTP was normal in conditional $Ca_V1.2$ knockout mice (Fig 9D–F). Accordingly, respective NMDAR-dependent synaptic plasticity mechanisms can be engaged in a normal manner in the $Ca_V1.2$ knockout mice when PTT-LTP is absent. Strikingly, Myr-Pep2 but not Myr-Pep2scr blocked PTT-LTP in wild-type mice (Fig 9G–I).

Discussion

The importance of tight control over β_2AR signaling is exemplified by the existence of a complex set of distinct mechanisms for its down-regulation upon prolonged activation (Shenoy & Lefkowitz, 2011), which include receptor phosphorylation by G protein-coupled receptor kinases (GRKs) (Nobles *et al*, 2011) and the consequent phosphorylation-triggered recruitment of arrestins for receptor uncoupling from Gs and endocytosis (Lohse *et al*, 1990; von Zastrow & Kobilka, 1992; Ferguson *et al*, 1996; Goodman *et al*, 1996; Cao *et al*, 1999) as well as the activity-dependent, PKA-mediated switching of β_2AR coupling from Gs to Gi (Daaka *et al*, 1997; Xiao *et al*, 1999a). Our surprising discovery of the role of S1928 phosphorylation in displacing the β_2AR unveils a novel negative feedback regulatory mechanism that targets the pervasive regulation of $Ca_v1.2$ by the β_2AR to prevent excessive Ca^{2+} influx into neurons. This mechanism is

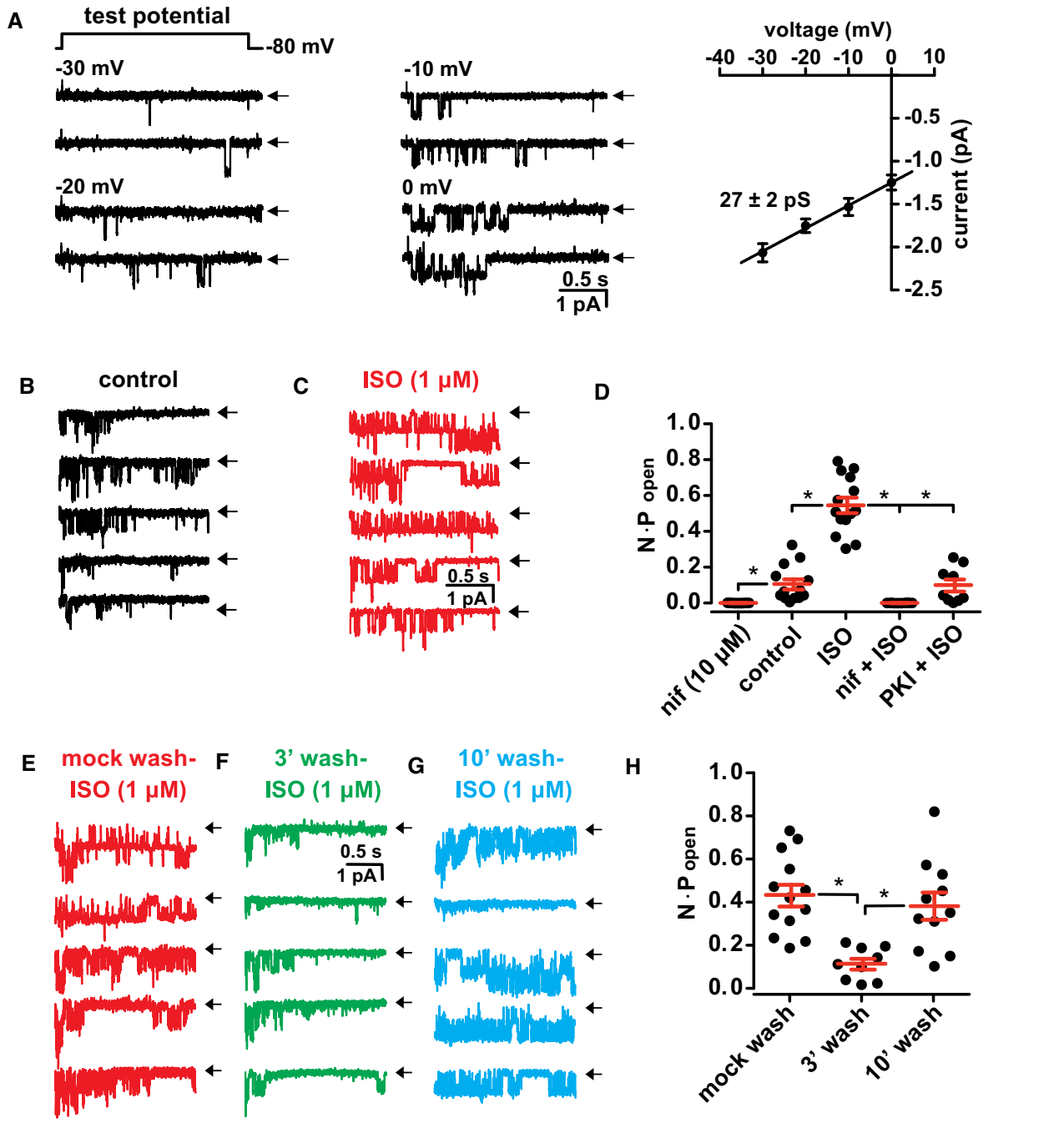

Figure 7. ISO-induced displacement of the β_2AR from $Ca_V1.2$ blunts subsequent stimulation of L-type channel activity.

A Representative single-channel recordings from hippocampal neurons at 7–14 DIV with 500 nM BayK-8644, 1 μM ω-conotoxin GVIA, and 1 μM MVIIC in patch pipette upon depolarization from −80 to −30, −20, −10, and 0 mV. The right panel depicts the single-channel current–voltage relationship. Mean amplitude of unitary currents for different membrane potential studied are −2.07 pA (−30 mV), −1.75 (−20 mV), −1.53 (−10 mV), and −1.25 (0 mV; n = 5 patches per test potential). Solid line represents best-fit of data using a linear equation (R^2 = 0.92) revealing a slope conductance for these channels of 27 ± 2 pS.

B–D Representative single-channel traces and summary plot upon depolarization from −80 to 0 mV under control conditions and in the presence of ISO in the patch pipette. Cultures were pre-incubated for 15 min with 10 μM 11R-PKI if indicated. The patch pipette contained either vehicle for control, nifedipine (nif; 1 μM), ISO (1 μM), or ISO plus nifedipine, which blocked all currents. The ISO-induced increase in NPo was prevented by 11R-PKI.

E–H Representative single-channel currents upon depolarization from −80 to 0 mV and summary plot after pre-treatment of whole cultures with ISO. Cultures were pre-incubated with vehicle (H_2O, mock wash, E) or 1 μM ISO for 5 min (F, G) and washed for 3 (E, F) or 10 min (G) before forming the cell-attached patch with ISO present in the patch pipette. The upregulation of NPo to ~0.4 (cf. C, D) occurred only if neurons were pretreated with vehicle instead of ISO (E, H; mock wash) or if ISO washout duration was 10 min (G, H) but not if washout was only 3 min (F, H).

Data information: Data are presented as mean ± SEM. NPo was determined for each recording and pooled under each condition for comparison (n = 10–14 patches; *P < 0.05, one-way ANOVA with Tukey *post hoc* test). Arrows throughout the figure indicate the 0-current level (i.e., closed channel).

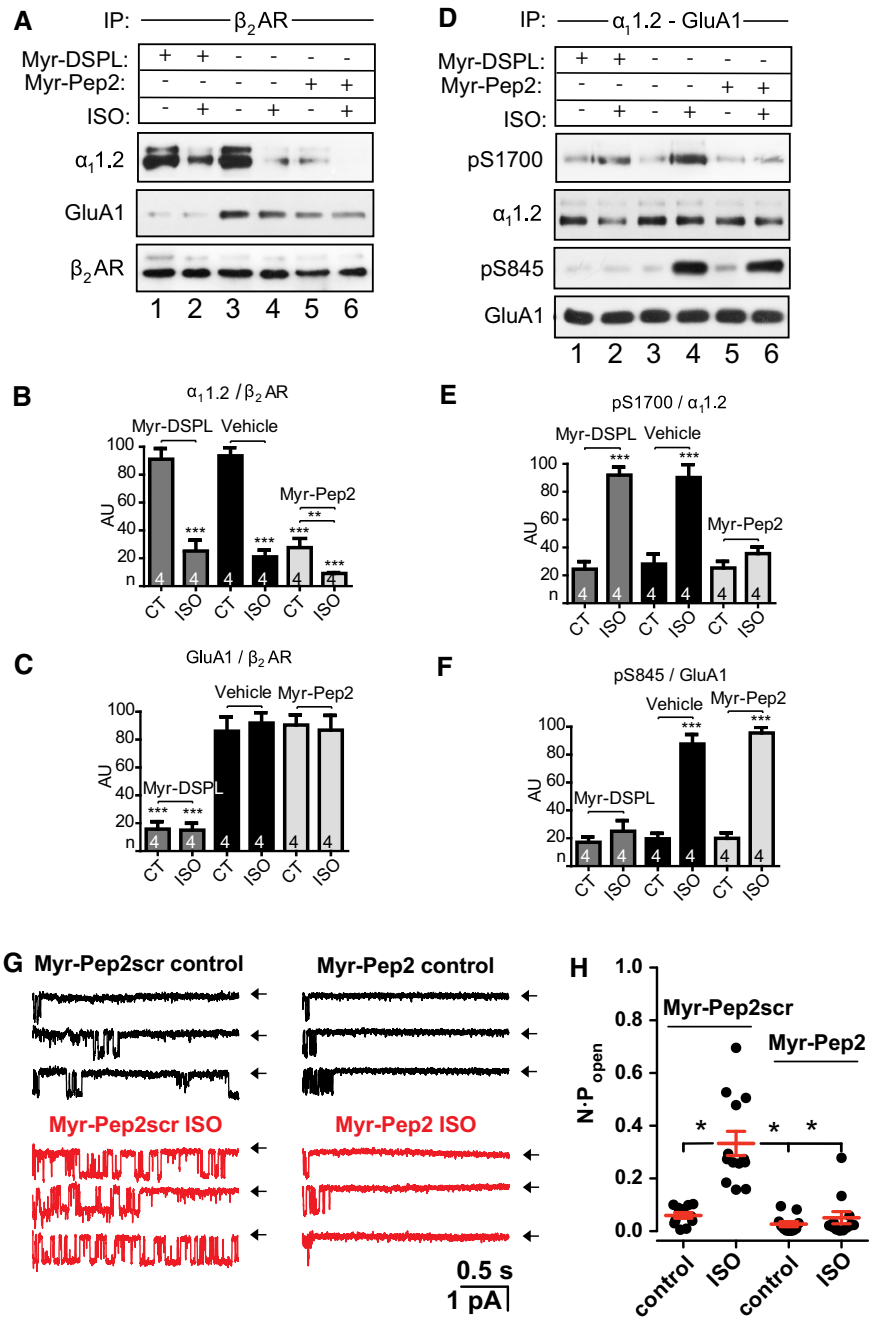

Figure 8. β_2AR binding to $\alpha_1$1.2 is required for β-adrenergic stimulation of $\alpha_1$1.2 phosphorylation and L-type currents.

Forebrain slices (A–F) were pre-incubated for 30 min with vehicle (water) or 10 μM Myr-Pep2 or Myr-DSPL. Like Myr-DSPL (Joiner *et al*, 2010), Pep2 was myristoylated at its N-terminus (Myr-Pep2) to make it membrane permeant. Slices were then treated with ISO (10 μM, 5 min) or vehicle (water) before solubilization, ultracentrifugation, and IP of β_2AR (A–C) or simultaneously $\alpha_1$1.2 and GluA1 with a combination of corresponding antibodies within same samples (D–F).

A Myr-Pep 2 displaced $\alpha_1$1.2 (lane 5 vs. 3, top of blot) but not GluA1 (middle, same blot) from β_2AR (bottom, same blot); the inverse was true for Myr-DSPL (lane 1 vs. 3).

B, C For quantification, $\alpha_1$1.2 (B) and GluA1 (C) immunosignals from (A) were normalized to β_2AR signals.

D Myr-Pep2 blunted ISO-induced phosphorylation of $\alpha_1$1.2 S1700 (lane 6 vs. 4, top of blot) but not GluA1 S845 (middle, same blot); the inverse was true for Myr-DSPL (lane 2 vs. 4).

E, F For quantification, pS1700 (E) and pS845 (F) immunosignals from (D) were normalized to $\alpha_1$1.2 and GluA1 signals, respectively.

G Representative cell-attached recordings from hippocampal neurons as in Fig 7. In interleafed experiments, cultures were pre-incubated for 30 min with 10 μM Myr-Pep2 or scrambled Myr-Pep2 (Myr-Pep2scr). The patch pipette contained either vehicle (H_2O; control) or 1 μM ISO. The ISO-induced increase in NPo was prevented by Myr-Pep2 but not Myr-Pep2scr. Arrows indicate the 0-current level (i.e., closed channel).

H Summary plot for (G). For statistical analysis, the NPo value was determined for each recording and pooled under each condition for comparison.

Data information: Data are presented as mean ± SEM. (B, C, E, F): $n = 4$. $^{**}P < 0.01$, $^{***}P < 0.001$, one-way ANOVA. (H): $n = 10$–12 patches; $^{*}P < 0.005$, one-way Tukey *post hoc* test.

devoted to highly specific downregulation of β_2AR signaling to $Ca_v1.2$ but not AMPARs, revealing how tightly controlled the activity of $Ca_v1.2$ must be to ensure proper function.

Our first important finding is that phosphorylation of S1928 in $\alpha_1$1.2 displaces the β_2AR from the C-terminus of $Ca_v1.2$. S1928 is the most prominent PKA phosphorylation site in $Ca_v1.2$ as determined

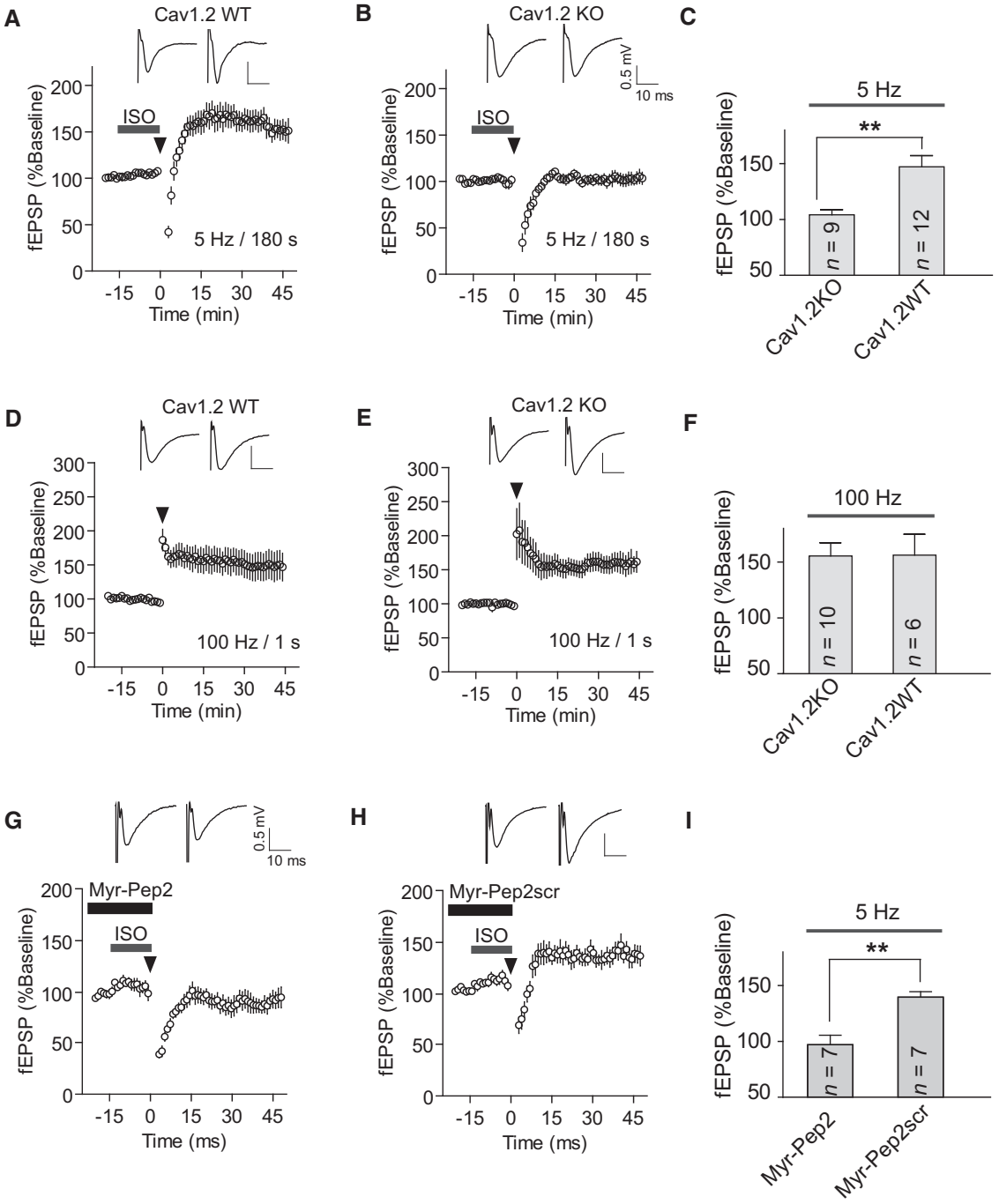

Figure 9. β_2AR binding to $\alpha_1$1.2 is required for PTT-LTP.

Graphs depict fEPSP initial slopes recorded from hippocampal CA1 before and after either a 5 Hz/3 min (A–C, G–I) or 100 Hz/1 s tetanus (D–F). Arrowheads mark onset of tetani and bars perfusion with 1 μM ISO and 10 μM of Myr-Pep2 or Myr-Pep2scr. Inserts show sample traces immediately before (left) and ~30 min after (right) tetani.

A–C Litter-matched WT but not conditional $Ca_v1.2$ KO mice showed PTT-LTP.

D–F WT as well as $Ca_v1.2$ KO mice showed NMDAR-dependent 100 Hz LTP.

G–I Myr-Pep2 but not Myr-Pep2scr blocked PTT-LTP.

Data information: Data are presented as mean ± SEM. $^{**}P < 0.01$, one-way ANOVA.

by biochemical methods, and S1928 phosphorylation is robustly induced by β adrenergic signaling (Hell *et al*, 1993b, 1995; De Jongh *et al*, 1996; Davare *et al*, 1999, 2000; Davare & Hell, 2003; Hulme *et al*, 2006a; Hall *et al*, 2007; Dai *et al*, 2009). However, its physiological role has remained an enigma, as it does not appear to significantly augment channel function in the heart (Ganesan *et al*, 2006; Lemke *et al*, 2008), which is mediated in part by phosphorylation of S1700 (Fuller *et al*, 2010; Hell, 2010; Fu *et al*, 2013, 2014). We now identify S1928 phosphorylation as a novel negative feedback mechanism for $Ca_v1.2$ regulation by β_2AR signaling. This is the first example of termination of G_sPCR activity by dissociation of a receptor–substrate complex and therefore introduces a new paradigm for the regulation of cell signaling by this widely expressed class of receptors.

Our second important finding is that dissociation of the β_2AR–$Ca_v1.2$ interaction by either S1928 phosphorylation during an initial ISO treatment or by Myr-Pep2 prevents upregulation of channel phosphorylation and activity by subsequent ISO application. Could ISO-induced displacement of the β_2AR from $Ca_v1.2$ result in endocytosis of the β_2AR, making it inaccessible to ISO and therefore to regulation? Evidently that is not the case, as abrogation of the re-phosphorylation of S1700 and S1928 during a second ISO application within 3 min of the initial one was not affected by dynasore or pitstop (Fig EV3), two different endocytosis inhibitors whose efficacy is well established in our hands (Hall *et al*, 2013). Accordingly, preventing β_2AR endocytosis, which in some cell lines is a general mechanism of downregulating signaling through the β_2AR (von Zastrow & Kobilka, 1992; Cao *et al*, 1999; Shenoy & Lefkowitz, 2011), does not affect this $Ca_v1.2$-specific form of downregulation. We conclude that it is the displacement of the β_2AR from $Ca_v1.2$ *per se* that is responsible for loss of subsequent signaling and not endocytosis of this receptor. This conclusion is also in accordance with the finding that the β_2AR can fully re-associate with $Ca_v1.2$ within 10 min (Figs 5A and B, and EV2A and C). Re-association of the β_2AR with $Ca_v1.2$ was paralleled by the ability of a second ISO application to induce re-phosphorylation of S1700 and S1928 (Fig EV3A, lane 3, and C). This finding underlines the notions that ISO-induced displacement of the β_2AR from $Ca_v1.2$ is not permanent and that the functionality of this interaction is reinstated within minutes.

Our third important finding is that displacement of the β_2AR from $Ca_v1.2$ is a specific process that downregulates signaling from the β_2AR to $Ca_v1.2$ without affecting β_2AR-mediated regulation of GluA1, which also forms a signaling complex with the β_2AR. This mechanism is fundamentally different from the arrestin-mediated downregulation of β_2AR signaling by endocytosis and by uncoupling from Gs (Shenoy & Lefkowitz, 2011). Most strikingly, downregulation of $Ca_v1.2$ stimulation is highly specific for $Ca_v1.2$, whereas arrestin-mediated effects are cell-wide affecting all β_2AR signaling. On a molecular level, arrestin is recruited to stimulated β_2ARs upon their phosphorylation by GRKs, whereas the PKA-mediated phosphorylation of S1928 acts to displace the β_2AR from $Ca_v1.2$.

Our fourth important finding is that PTT-LTP depends on $Ca_v1.2$ and its association of the β_2AR. PTT-LTP is induced by prolonged stimulation at 5 Hz, which approximates the naturally occurring θ rhythm in the hippocampus (Mizuseki *et al*, 2009). Prolonged stimulation at the naturally occurring theta tetanus induces LTP (PTT-LTP) if at the same time β adrenergic signaling is engaged (Thomas *et al*, 1996; Hu *et al*, 2007; Qian *et al*, 2012). PTT-LTP is thought to be important for contextual learning under demanding situations (Hu *et al*, 2007). The β_2AR–$Ca_v1.2$ signaling cascade might thus be important for such learning.

The finding that the association of the β_2AR with $Ca_v1.2$ is critical for β adrenergic regulation of $Ca_v1.2$ has important further functional implications. Accordingly, the β_2AR must be localized in the immediate vicinity of $Ca_v1.2$ for effective signaling. This signaling is clearly mediated by the cAMP/PKA cascade as the PKA-specific inhibitory PKI peptide prevented the ISO-induced upregulation of L-type currents (Fig 7D). Loss of cAMP signaling from the β_2AR to $Ca_v1.2$ upon their dissociation constitutes the first clear evidence for the hypothesis that cAMP signaling by certain GsPCR, especially the paradigmatic β_2AR (Kuschel *et al*, 1999; Chen-Izu *et al*, 2000; Davare *et al*, 2001; Balijepalli *et al*, 2006; Nikolaev *et al*, 2010), is mediated by cAMP production that is localized within nanodomains, that is, domains smaller than 100 nm in diameter. The reasoning for this notion is that the average distance between more or less evenly distributed β_2ARs on the cell surface will not allow for regions devoid of β_2ARs that are larger than 100 nm; likely, such regions are much smaller. We also exclude that ISO-triggered endocytosis is playing a role in functional uncoupling of the β_2AR from regulating $Ca_v1.2$ phosphorylation (Fig EV3). The localized regulation of $Ca_v1.2$ via cAMP signaling is consistent with earlier finding that in addition to AKAP150-anchored PKA (Hall *et al*, 2007; Oliveria *et al*, 2007; Dittmer *et al*, 2014), G_s and adenylyl cyclase are also associated with $Ca_v1.2$ (Davare *et al*, 2001; Balijepalli *et al*, 2006).

Downregulation of β adrenergic augmentation of $Ca_v1.2$ activity might provide a brake necessary to ensure cell integrity, which could be jeopardized by the otherwise overpowering effects of a sustained increase in Ca^{2+} influx. In contrast, continued upregulation of GluA1 phosphorylation by prolonged β adrenergic stimulation might not be as detrimental because these receptors primarily conduct Na^+ rather than Ca^{2+}.

In conclusion, we demonstrate that S1928 phosphorylation of $Ca_v1.2$ upon β_2AR stimulation results in a temporary dissociation of the β_2AR from $Ca_v1.2$ with an equally fleeting but complete loss of $Ca_v1.2$ regulation by the β_2AR. This novel potent negative feedback mechanism adds to the surprisingly diverse arsenal of tools the cell developed to curb overactivation of βAR signaling and $Ca_v1.2$.

Materials and Methods

Animals

All procedures followed NIH guidelines and had been approved by the IACUC at UC Davis. S1928A KI mice were described by Lemke *et al* (2008) and conditional forebrain $Ca_v1.2$ KO mice by White *et al* (2008). All mice used in this study were between 8 and 12 weeks old.

Reagents, peptides, and antibodies

Isoproterenol bitartrate salt, ICI118551, CGP20712, and microcystin LR were from Sigma. Dynasore was from Tocris and Pitstop from Abcam. Protein A-covered beads were from Repligen and Amylose beads from New England Biolabs. Polyvinyldifluoride (PVDF)

membranes were from Millipore. Horseradish peroxidase-coupled (HRP) protein A, ECL, and ECL plus reagents were from GE Healthcare. The chemiluminescent Femto substrate, EGTA, EDTA, Tween-20, Triton X-100, and tris(hydroxymethyl)aminomethane (Tris) were from Fisher Thermo Scientific. Other reagents were from the typical suppliers and of the usual quality.

All synthetic peptides (Appendix Table S1) were purchased from China Peptides (Shanghai, China). Origin and other details of antibodies are given in Appendix Table S2.

Fluorescence polarization (FP)

Fluorescein (FITC)-labeled synthetic peptides (1 μM final conc.) were added to serial dilutions (8 times twofold, i.e., each time 1:1) of recombinant MBP-tagged β_2AR C-terminus in FP buffer (50 mM HEPES, 100 mM KCl, 1 mM $MgCl_2$, 0.05 mM EGTA, 5 mM NTA, pH 7.4) in black 384-well polystyrene plates (Corning). FP was measured with a Synergy 2 (BioTek) plate reader with polarization filters to determine parallel and perpendicular fluorescence intensities of exciting (485/20λ) and emitted light (528/20λ). Data were acquired with Gen5 software. FP was calculated as $P = (I_v - g*I_h)/(I_v + g*I_h)$; I_v and I_h constitute the vertical and horizontal fluorescence intensities, respectively, and g the correction factor for fluorescein. Data were analyzed with GraphPad Prism 5 for curve fitting and K_d determination by fitting binding curves to the equation $Y = B*X/(K_d + X)$; B is the maximal FP value that would be reached at saturation as determined by extrapolation of the fitted curve (Lim *et al*, 2002).

Preparation of brain slices and use for biochemical analysis

Mice (8–12 weeks) were decapitated and brains placed into ice-cold artificial cerebrospinal fluid (ACSF; in mM: 127 NaCl, 26 $NaHCO_2$, 1.2 KH_2PO_4, 1.9 KCl, 2.2 $CaCl_2$, 1 $MgSO_4$ and 10 D-glucose, 290–300 mOsm/kg, saturated with 95% O_2, and 5% CO_2; final pH 7.3). About one-third of the rostral and caudal ends of the brain were trimmed off. A total of 350-μm-thick forebrain slices containing hippocampus were prepared with a vibratome (Leica VT 1000A). Slices were equilibrated in oxygenated ACSF for 1 h at 30°C before transfer to incubation chambers, equilibration for 30 min at 32°C and treatment with vehicle (H_2O), ISO (10 μM). Slices were extracted with IP buffer containing protease and phosphatase inhibitors as above before IP of β_2AR, $\alpha_1$1.2, and anti-GluA1 and IB as above.

Methods for immunoprecipitation (IP) and immunoblotting (IB) as well as pull-down and fluorescence microscopy are standard, and details are given in Appendix Supplementary Methods. The $Ca_v1.2$ glutathione S-transferase (GST)-fusion proteins of $\alpha_1$1.2 are described in Hall *et al* (2006, 2007, 2013) and listed in Appendix Table S3. The maltose-binding protein (MBP)-tagged C-terminus (CT) of human β_2AR (residues 326–413) is as in Joiner *et al* (2010).

Electrophysiology

Cell-attached patch clamp recordings were performed as previously (Davare *et al*, 2001) with 500 nM (*S*)-(−)-BayK-8644, 1 μM ω-conotoxin GVIA, and 1 μM ω-conotoxin MCVIIC in the patch pipette. Hippocampal slice recordings were basically as described (Qian *et al*, 2012). Exact details are given in Appendix Supplementary Methods.

Expanded View for this article is available online.

Acknowledgements

We thank Dr. Brian K. Kobilka, Stanford University, California, USA, for the pcDNA3.1-FLAG-β_2AR construct and Angela Steinberger for providing primary cultures of hippocampal neurons and for excellent technical assistance. This work was supported by NIH grants R01 NS078792 and R01 MH097887 (JWH), R01 HL098200 and R01 HL121059 (MFN), R01 HL085372 (WAC), and R01 HL127764 (YKX), R01 AG028488 (GGM), American Heart Association (to YKX, who is an AHA Establish Investigator), Austrian Science Fund (FWF) grant P 25085 (VDB), and grants from Deutsche Forschungsgemeinschaft (FH).

Author contributions

TP, VDB, WAC, FH, YKX, GGM, CYC, MFN, and JWH designed experiments; TP, HQ, VDB, ZAM, DC, JLP, EAH, ORB, REW, CYC, and MFN performed experiments; TP, HQ, VDB, JLP, EAH, CYC, and MFN analyzed data; TP, MFN, and JWH wrote the manuscript.

Conflict of interest

The authors declare that they have no conflict of interest.

References

Balijepalli RC, Foell JD, Hall DD, Hell JW, Kamp TJ (2006) From the Cover: localization of cardiac L-type Ca2+ channels to a caveolar macromolecular signaling complex is required for beta2-adrenergic regulation. *Proc Natl Acad Sci USA* 103: 7500 – 7505

Berkefeld H, Sailer CA, Bildl W, Rohde V, Thumfart JO, Eble S, Klugbauer N, Reisinger E, Bischofberger J, Oliver D, Knaus HG, Schulte U, Fakler B (2006) BKCa-Cav channel complexes mediate rapid and localized Ca2+-activated K+ signaling. *Science* 314: 615 – 620

Berman DE, Dudai Y (2001) Memory extinction, learning anew, and learning the new: dissociations in the molecular machinery of learning in cortex. *Science* 291: 2417 – 2419

Bolshakov VY, Siegelbaum SA (1994) Postsynaptic induction and presynaptic expression of hippocampal long-term depression. *Science* 264: 148 – 152

Cahill L, Prins B, Weber M, McGaugh JL (1994) Beta-adrenergic activation and memory for emotional events. *Nature* 371: 702 – 704

Cao TT, Deacon HW, Reczek D, Bretscher A, von Zastrow M (1999) A kinase-regulated PDZ-domain interaction controls endocytic sorting of the beta2-adrenergic receptor. *Nature* 401: 286 – 290

Carter ME, Yizhar O, Chikahisa S, Nguyen H, Adamantidis A, Nishino S, Deisseroth K, de Lecea L (2010) Tuning arousal with optogenetic modulation of locus coeruleus neurons. *Nature Neurosci* 13: 1526 – 1533

Chen-Izu Y, Xiao RP, Izu LT, Cheng H, Kuschel M, Spurgeon H, Lakatta EG (2000) G(i)-dependent localization of beta(2)-adrenergic receptor signaling to L-type Ca(2+) channels. *Biophys J* 79: 2547 – 2556

Daaka Y, Luttrell LM, Lefkowitz RJ (1997) Switching of the coupling of the beta2-adrenergic receptor to different G proteins by protein kinase A. *Nature* 390: 88 – 91

Dai S, Hall DD, Hell JW (2009) Supramolecular Assemblies and Localized Regulation of Voltage-gated Ion Channels. *Physiol Rev* 89: 411 – 452

Davare MA, Avdonin V, Hall DD, Peden EM, Burette A, Weinberg RJ, Horne MC, Hoshi T, Hell JW (2001) A beta2 adrenergic receptor signaling complex assembled with the Ca2+ channel Cav1.2. *Science* 293: 98 – 101

Davare MA, Dong F, Rubin CS, Hell JW (1999) The A-kinase anchor protein MAP2B and cAMP-dependent protein kinase are associated with class C L-type calcium channels in neurons. *J Biol Chem* 274: 30280 – 30287

Davare MA, Hell JW (2003) Increased phosphorylation of the neuronal L-type Ca(2+) channel Ca(v)1.2 during aging. *Proc Natl Acad Sci USA* 100: 16018 – 16023

Davare MA, Horne MC, Hell JW (2000) Protein Phosphatase 2A is associated with class C L-type calcium channels ($Ca_v1.2$) and antagonizes channel phosphorylation by cAMP-dependent protein kinase. *J Biol Chem* 275: 39710 – 39717

De Jongh KS, Murphy BJ, Colvin AA, Hell JW, Takahashi M, Catterall WA (1996) Specific phosphorylation of a site in the full length form of the a1 subunit of the cardiac L-type calcium channel by adenosine 3′,5′-cyclic monophosphate-dependent protein kinase. *Biochem* 35: 10392 – 10402

Dittmer PJ, Dell'Acqua ML, Sather WA (2014) Ca(2+)/Calcineurin-Dependent Inactivation of Neuronal L-Type Ca(2+) Channels Requires Priming by AKAP-Anchored Protein Kinase A. *Cell Rep* 7: 1410 – 1416

Dolmetsch RE, Pajvani U, Fife K, Spotts JM, Greenberg ME (2001) Signaling to the nucleus by an L-type calcium channel-calmodulin complex through the MAP kinase pathway. *Science* 294: 333 – 339

Efendiev R, Samelson BK, Nguyen BT, Phatarpekar PV, Baameur F, Scott JD, Dessauer CW (2010) AKAP79 interacts with multiple adenylyl cyclase (AC) isoforms and scaffolds AC5 and -6 to alpha-amino-3-hydroxyl-5-methyl-4-isoxazole-propionate (AMPA) receptors. *J Biol Chem* 285: 14450 – 14458

Ferguson SS, Downey WE 3rd, Colapietro AM, Barak LS, Menard L, Caron MG (1996) Role of beta-arrestin in mediating agonist-promoted G protein-coupled receptor internalization. *Science* 271: 363 – 366

Fu Y, Westenbroek RE, Scheuer T, Catterall WA (2013) Phosphorylation sites required for regulation of cardiac calcium channels in the fight-or-flight response. *Proc Natl Acad Sci USA* 110: 19621 – 19626

Fu Y, Westenbroek RE, Scheuer T, Catterall WA (2014) Basal and beta-adrenergic regulation of the cardiac calcium channel CaV1.2 requires phosphorylation of serine 1700. *Proc Natl Acad Sci USA* 111: 16598 – 16603

Fuller MD, Emrick MA, Sadilek M, Scheuer T, Catterall WA (2010) Molecular mechanism of calcium channel regulation in the fight-or-flight response. *Sci Signal* 3: ra70

Fuller MD, Fu Y, Scheuer T, Catterall WA (2014) Differential regulation of CaV1.2 channels by cAMP-dependent protein kinase bound to A-kinase anchoring proteins 15 and 79/150. *J Gen Physiol* 143: 315 – 324

Ganesan AN, Maack C, Johns DC, Sidor A, O'Rourke B (2006) Beta-adrenergic stimulation of L-type Ca2+ channels in cardiac myocytes requires the distal carboxyl terminus of alpha1C but not serine 1928. *Circ Res* 98: e11 – e18

Goodman OB Jr, Krupnick JG, Santini F, Gurevich VV, Penn RB, Gagnon AW, Keen JH, Benovic JL (1996) Beta-arrestin acts as a clathrin adaptor in endocytosis of the beta2-adrenergic receptor. *Nature* 383: 447 – 450

Gray R, Johnston D (1987) Noradrenaline and beta-adrenoceptor agonists increase activity of voltage-dependent calcium channels in hippocampal neurons. *Nature* 327: 620 – 622

Grover LM, Teyler TJ (1990) Two components of long-term potentiation induced by different patterns of afferent activation. *Nature* 347: 477 – 479

Hall DD, Dai S, Tseng P-Y, Malik ZA, Nguyen M, Matt L, Schnizler K, Shephard A, Mohapatra D, Tsuruta F, Dolmetsch RE, Christel CJ, Lee A, Burette A, Weinberg RJ, Hell JW (2013) Competition Between α-Actinin and Ca2+-Calmodulin Controls Surface Retention of the L-type Ca2+ Channel CaV1.2. *Neuron* 78: 483 – 497

Hall DD, Davare MA, Shi M, Allen ML, Weisenhaus M, McKnight GS, Hell JW (2007) Critical role of cAMP-dependent protein kinase anchoring to the L-type calcium channel Cav1.2 via A-kinase anchor protein 150 in neurons. *Biochem* 46: 1635 – 1646

Hall DD, Feekes JA, Arachchige Don AS, Shi M, Hamid J, Chen L, Strack S, Zamponi GW, Horne MC, Hell JW (2006) Binding of protein phosphatase 2A to the L-type calcium channel Cav1.2 next to Ser 1928, its main PKA site, is critical for Ser1928 dephosphorylation. *Biochem* 45: 3448 – 3459

Halt AR, Dallapiazza R, Yu H, Stein IS, Qian H, Junti S, Wojcik S, Brose N, Sliva A, Hell JW (2012) CaMKII binding to GluN2B is Critical During Memory Consolidation. *EMBO J* 31: 1203 – 1216

Hell JW (2010) {beta}-adrenergic regulation of the L-Type Ca2+ channel CaV1.2 by PKA rekindles excitement. *Sci Signal* 3: pe33

Hell JW, Westenbroek RE, Warner C, Ahlijanian MK, Prystay W, Gilbert MM, Snutch TP, Catterall WA (1993a) Identification and differential subcellular localization of the neuronal class C and class D L-type calcium channel a1 subunits. *J Cell Biol* 123: 949 – 962

Hell JW, Yokoyama CT, Breeze LJ, Chavkin C, Catterall WA (1995) Phosphorylation of presynaptic and postsynaptic calcium channels by cAMP-dependent protein kinase in hippocampal neurons. *EMBO J* 14: 3036 – 3044

Hell JW, Yokoyama CT, Wong ST, Warner C, Snutch TP, Catterall WA (1993b) Differential phosphorylation of two size forms of the neuronal class C L-type calcium channel a1 subunit. *J Biol Chem* 268: 19451 – 19457

Hoogland TM, Saggau P (2004) Facilitation of L-type Ca2+ channels in dendritic spines by activation of beta2 adrenergic receptors. *J Neurosci* 24: 8416 – 8427

Hu H, Real E, Takamiya K, Kang MG, Ledoux J, Huganir RL, Malinow R (2007) Emotion Enhances Learning via Norepinephrine Regulation of AMPA-Receptor Trafficking. *Cell* 131: 160 – 173

Hulme JT, Lin TW, Westenbroek RE, Scheuer T, Catterall WA (2003) Beta-adrenergic regulation requires direct anchoring of PKA to cardiac CaV1.2 channels via a leucine zipper interaction with A kinase-anchoring protein 15. *Proc Natl Acad Sci USA* 100: 13093 – 13098

Hulme JT, Westenbroek RE, Scheuer T, Catterall WA (2006a) Phosphorylation of serine 1928 in the distal C-terminal domain of cardiac CaV1.2 channels during beta1-adrenergic regulation. *Proc Natl Acad Sci USA* 103: 16574 – 16579

Hulme JT, Yarov-Yarovoy V, Lin TW, Scheuer T, Catterall WA (2006b) Autoinhibitory Control of the CaV1.2 Channel by its Proteolytically Processed Distal C-terminal Domain. *J Physiol* 576: 87 – 102

Joiner ML, Lise MF, Yuen EY, Kam AY, Zhang M, Hall DD, Malik ZA, Qian H, Chen Y, Ulrich JD, Burette AC, Weinberg RJ, Law PY, El-Husseini A, Yan Z, Hell JW (2010) Assembly of a beta(2)-adrenergic receptor-GluR1 signalling complex for localized cAMP signalling. *EMBO J* 29: 482 – 495

Jurevicius J, Fischmeister R (1996) cAMP compartmentation is responsible for a local activation of cardiac Ca2+ channels by beta-adrenergic agonists. *Proc Natl Acad Sci USA* 93: 295 – 299

Kuschel M, Zhou YY, Cheng H, Zhang SJ, Chen Y, Lakatta EG, Xiao RP (1999) G (i) protein-mediated functional compartmentalization of cardiac beta(2)-adrenergic signaling. *J Biol Chem* 274: 22048 – 22052

Lemke T, Welling A, Christel CJ, Blaich A, Bernhard D, Lenhardt P, Hofmann F, Moosmang S (2008) Unchanged beta-adrenergic stimulation of cardiac L-type calcium channels in Ca v 1.2 phosphorylation site S1928A mutant mice. *J Biol Chem* 283: 34738 – 34744

Leonard AS, Davare MA, Horne MC, Garner CC, Hell JW (1998) SAP97 is associated with the a-amino-3-hydroxy-5-methylisoxazole-4-propionic acid receptor GluR1 subunit. *J Biol Chem* 273: 19518 – 19524

Leroy J, Abi-Gerges A, Nikolaev VO, Richter W, Lechene P, Mazet JL, Conti M, Fischmeister R, Vandecasteele G (2008) Spatiotemporal dynamics of beta-adrenergic cAMP signals and L-type Ca2+ channel regulation in adult rat ventricular myocytes: role of phosphodiesterases. *Circ Res* 102: 1091 – 1100

Li H, Pink MD, Murphy JG, Stein A, Dell'Acqua ML, Hogan PG (2012) Balanced interactions of calcineurin with AKAP79 regulate Ca2+-calcineurin-NFAT signaling. *Nat Struct Mol Biol* 19: 337 – 345

Lim IA, Hall DD, Hell JW (2002) Selectivity and promiscuity of the first and second PDZ domains of PSD- 95 and synapse-associated protein 102. *J Biol Chem* 277: 21697 – 21711

Lohse MJ, Benovic JL, Codina J, Caron MG, Lefkowitz RJ (1990) beta-Arrestin: a protein that regulates beta-adrenergic receptor function. *Science* 248: 1547 – 1550

Lu Y, Allen M, Halt AR, Weisenhaus M, Dallapiazza RF, Hall DD, Usachev YM, McKnight GS, Hell JW (2007) Age-dependent requirement of AKAP150-anchored PKA and GluR2-lacking AMPA receptors in LTP. *EMBO J* 26: 4879 – 4890

Lu Y, Zha XM, Kim EY, Schachtele S, Dailey ME, Hall DD, Strack S, Green SH, Hoffman DA, Hell JW (2011) A kinase anchor protein150 (AKAP150)-associated protein kinase A limits dendritic spine density. *J Biol Chem* 286: 26496 – 26506

Ma H, Groth RD, Cohen SM, Emery JF, Li B, Hoedt E, Zhang G, Neubert TA, Tsien RW (2014) gammaCaMKII Shuttles Ca(2+)/CaM to the Nucleus to Trigger CREB Phosphorylation and Gene Expression. *Cell* 159: 281 – 294

Marrion NV, Tavalin ST (1998) Selective activation of Ca^{2+}-activated K^+ channels by co-localized Ca^{2+} channels in hippocampal neurons. *Nature* 395: 900 – 905

Marshall MR, Clark JP 3rd, Westenbroek R, Yu FH, Scheuer T, Catterall WA (2011) Functional roles of a C-terminal signaling complex of CaV1 channels and A-kinase anchoring protein 15 in brain neurons. *J Biol Chem* 286: 12627 – 12639

Minzenberg MJ, Watrous AJ, Yoon JH, Ursu S, Carter CS (2008) Modafinil shifts human locus coeruleus to low-tonic, high-phasic activity during functional MRI. *Science* 322: 1700 – 1702

Mizuseki K, Sirota A, Pastalkova E, Buzsaki G (2009) Theta oscillations provide temporal windows for local circuit computation in the entorhinal-hippocampal loop. *Neuron* 64: 267 – 280

Moosmang S, Haider N, Klugbauer N, Adelsberger H, Langwieser N, Muller J, Stiess M, Marais E, Schulla V, Lacinova L, Goebbels S, Nave KA, Storm DR, Hofmann F, Kleppisch T (2005) Role of hippocampal Cav1.2 Ca2+ channels in NMDA receptor-independent synaptic plasticity and spatial memory. *J Neurosci* 25: 9883 – 9892

Murphy JG, Sanderson JL, Gorski JA, Scott JD, Catterall WA, Sather WA, Dell'Acqua ML (2014). AKAP-anchored PKA maintains neuronal L-type calcium channel activity and NFAT transcriptional signaling. *Cell Rep* 7, 1577 – 1588

Nichols CB, Rossow CF, Navedo MF, Westenbroek RE, Catterall WA, Santana LF, McKnight GS (2010) Sympathetic stimulation of adult cardiomyocytes requires association of AKAP5 with a subpopulation of L-type calcium channels. *Circ Res* 107: 747 – 756

Nikolaev VO, Moshkov A, Lyon AR, Miragoli M, Novak P, Paur H, Lohse MJ, Korchev YE, Harding SE, Gorelik J (2010) Beta2-adrenergic receptor redistribution in heart failure changes cAMP compartmentation. *Science* 327: 1653 – 1657

Nobles KN, Xiao K, Ahn S, Shukla AK, Lam CM, Rajagopal S, Strachan RT, Huang TY, Bressler EA, Hara MR, Shenoy SK, Gygi SP, Lefkowitz RJ (2011) Distinct phosphorylation sites on the beta(2)-adrenergic receptor establish a barcode that encodes differential functions of beta-arrestin. *Sci Signal* 4: ra51

Oliveria SF, Dell'acqua ML, Sather WA (2007) AKAP79/150 anchoring of calcineurin controls neuronal L-Type Ca(2+) channel activity and nuclear signaling. *Neuron* 55: 261 – 275

Qian H, Matt L, Zhang M, Nguyen M, Patriarchi T, Koval ON, Anderson ME, He K, Lee H-K, Hell JW (2012) β2 Adrenergic Receptor Supports Prolonged Theta Tetanus - induced LTP. *J Neurophysiol* 107: 2703 – 2712

Reuter H (1983) Calcium channel modulation by neurotransmitters, enzymes and drugs. *Nature* 301: 569 – 574

Richter W, Mika D, Blanchard E, Day P, Conti M (2013) beta1-adrenergic receptor antagonists signal via PDE4 translocation. *EMBO Rep* 14: 276 – 283

Roche KW, O'Brien RJ, Mammen AL, Bernhardt J, Huganir RL (1996) Characterization of multiple phosphorylation sites on the AMPA receptor GluR1 subunit. *Neuron* 16: 1179 – 1188

Sanderson JL, Dell'Acqua ML (2011) AKAP signaling complexes in regulation of excitatory synaptic plasticity. *Neuroscientist* 17: 321 – 336

Shenoy SK, Lefkowitz RJ (2011) beta-Arrestin-mediated receptor trafficking and signal transduction. *Trends Pharmacol Sci* 32: 521 – 533

Smith FD, Langeberg LK, Scott JD (2006) The where's and when's of kinase anchoring. *Trends Biochem Sci* 31: 316 – 323

Splawski I, Timothy KW, Sharpe LM, Decher N, Kumar P, Bloise R, Napolitano C, Schwartz PJ, Joseph RM, Condouris K, Tager-Flusberg H, Priori SG, Sanguinetti MC, Keating MT (2004) Ca(V)1.2 calcium channel dysfunction causes a multisystem disorder including arrhythmia and autism. *Cell* 119: 19 – 31

Steinberg SF, Brunton LL (2001) Compartmentation of G protein-coupled signaling pathways in cardiac myocytes. *Annu Rev Pharmacol Toxicol* 41: 751 – 773

Tavalin SJ, Colledge M, Hell JW, Langeberg LK, Huganir RL, Scott JD (2002) Regulation of GluR1 by the A-kinase anchoring protein 79 (AKAP79) signaling complex shares properties with long-term depression. *J Neurosci* 22: 3044 – 3051

Thomas MJ, Moody TD, Makhinson M, O'Dell TJ (1996) Activity-dependent beta-adrenergic modulation of low frequency stimulation induced LTP in the hippocampal CA1 region. *Neuron* 17: 475 – 482

Wang D, Govindaiah G, Liu R, De Arcangelis V, Cox CL, Xiang YK (2010) Binding of amyloid beta peptide to beta2 adrenergic receptor induces PKA-dependent AMPA receptor hyperactivity. *Faseb J* 24: 3511 – 3521

White JA, McKinney BC, John MC, Powers PA, Kamp TJ, Murphy GG (2008) Conditional forebrain deletion of the L-type calcium channel Ca V 1.2 disrupts remote spatial memories in mice. *Learn Mem* 15: 1 – 5

Xiao RP, Avdonin P, Zhou YY, Cheng H, Akhter SA, Eschenhagen T, Lefkowitz RJ, Koch WJ, Lakatta EG (1999a) Coupling of beta2-adrenoceptor to Gi proteins and its physiological relevance in murine cardiac myocytes. *Circ Res* 84: 43 – 52

Xiao RP, Cheng H, Zhou YY, Kuschel M, Lakatta EG (1999b) Recent advances in cardiac beta(2)-adrenergic signal transduction. *Circ Res* 85: 1092 – 1100

Yue DT, Marban E (1990) Permeation in the dihydropyridine-sensitive calcium channel. Multi-ion occupancy but no anomalous mole-fraction effect between Ba2+ and Ca2+. *J Gen Physiol* 95: 911 – 939

von Zastrow M, Kobilka BK (1992) Ligand-regulated internalization and recycling of human beta 2-adrenergic receptors between the plasma membrane and endosomes containing transferrin receptors. *J Biol Chem* 267: 3530 – 3538

Zhang M, Patriarchi T, Stein IS, Qian H, Matt L, Nguyen M, Xiang YK, Hell JW (2013) Adenylyl cyclase anchoring by a kinase anchor protein AKAP5 (AKAP79/150) is important for postsynaptic beta-adrenergic signaling. *J Biol Chem* 288: 17918 – 17931